Pathogen-Associated Molecular Pattern-Triggered Immunity Involves Proteolytic Degradation of Core Nonsense-Mediated mRNA Decay Factors During the Early Defense Response[OPEN]

Ho Won Jung,[a] Gagan Kumar Panigrahi,[b,c,d] Ga Young Jung,[a] Yu Jeong Lee,[a] Ki Hun Shin,[b,c] Annapurna Sahoo,[b,c] Eun Su Choi,[a] Eunji Lee,[a] Kyung Man Kim,[b,c] Seung Hwan Yang,[e] Jong-Seong Jeon,[f] Sung Chul Lee,[g] and Sang Hyon Kim[b,c,1]

[a] Department of Applied Bioscience, Dong-A University, Busan 49315, Korea
[b] Department of Biosciences and Bioinformatics, Myongji University, Yongin 17058, Korea
[c] RNA Genomics Center, Myongji University, Yongin 17058, Korea
[d] School of Applied Sciences, Centurion University of Technology and Management, Odisha 752050, India
[e] Department of Biotechnology, Chonnam National University, Yeosu 59626, Korea
[f] Graduate School of Biotechnology and Crop Biotech Institute, Kyung Hee University, Yongin 17104, Korea
[g] School of Biological Sciences, Chung-Ang University, Seoul 06974, Korea

ORCID IDs: 0000-0001-6408-4168 (H.W.J.); 0000-0003-3908-3379 (G.K.P.); 0000-0001-7829-3825 (G.Y.J.); 0000-0002-8145-9520 (Y.J.L.); 0000-0002-7530-6229 (K.H.S.); 0000-0002-5079-0261 (A.S.); 0000-0001-9503-6441 (E.S.C.); 0000-0001-6777-0876 (E.L.); 0000-0001-5105-922X (K.M.K.); 0000-0003-0603-2209 (S.H.Y.); 0000-0001-6221-4993 (J.-S.J.); 0000-0003-2725-0854 (S.C.L.); 0000-0003-3444-4446 (S.H.K.).

Nonsense-mediated mRNA decay (NMD), an mRNA quality control process, is thought to function in plant immunity. A subset of fully spliced (FS) transcripts of Arabidopsis (*Arabidopsis thaliana*) resistance (*R*) genes are upregulated during bacterial infection. Here, we report that 81.2% and 65.1% of FS natural TIR-NBS-LRR (TNL) and CC-NBS-LRR transcripts, respectively, retain characteristics of NMD regulation, as their transcript levels could be controlled posttranscriptionally. Both bacterial infection and the perception of bacteria by pattern recognition receptors initiated the destruction of core NMD factors UP-FRAMESHIFT1 (UPF1), UPF2, and UPF3 in Arabidopsis within 30 min of inoculation via the independent ubiquitination of UPF1 and UPF3 and their degradation via the 26S proteasome pathway. The induction of UPF1 and UPF3 ubiquitination was delayed in *mitogen-activated protein kinase3* (*mpk3*) and *mpk6*, but not in salicylic acid-signaling mutants, during the early immune response. Finally, previously uncharacterized TNL-type *R* transcripts accumulated in *upf* mutants and conferred disease resistance to infection with a virulent *Pseudomonas* strain in plants. Our findings demonstrate that NMD is one of the main regulatory processes through which PRRs fine-tune *R* transcript levels to reduce fitness costs and achieve effective immunity.

INTRODUCTION

Plant immunity, a counterattack mechanism against microbial infection, is exquisitely controlled by two different immune receptors known as extracellular immune receptors (pattern recognition receptors, PRRs) and intracellular immune receptors (resistance [R] proteins; nucleotide binding oligomerization domain–like receptors [NOD-like receptors or NLRs]; or nucleotide binding site–leucine-rich repeat [NBS-LRR] proteins) that recognize microbe-associated molecular patterns (MAMPs) and pathogen-derived effectors, respectively. In general, pattern-triggered immunity (PTI), which is controlled by PRRs, confers moderate disease resistance to a broad spectrum of pathogens, and effector-triggered immunity (ETI), which is controlled by R proteins, is responsible for resistance to a specific pathogen carrying a cognate avirulence gene (Chisholm et al., 2006; Jones and Dangl, 2006). In addition to their predominance, *R* genes are also indispensable for establishing basal immunity to virulent pathogen infection and maintaining the balance between growth and defense (Li et al., 2001; Shirano et al., 2002; Palma et al., 2010; Maekawa et al., 2011; Karasov et al., 2017). The maintenance of the switched-off state and posttranslational modification of R proteins by other cellular components are crucial for maintaining the proper homeostasis of R activity (DeYoung and Innes, 2006; Li et al., 2015; Karasov et al., 2017). Transcriptional controls, such as histone modification and DNA methylation, are fundamental for fine-tuning *R* transcript levels (Halter and Navarro, 2015; Lai and Eulgem, 2018). Alternative splicing (AS) can secure the accumulation of diverse transcript isoforms for full immunity (Dinesh-Kumar and Baker, 2000; Zhang and Gassmann, 2007; Xu et al., 2012; Yang et al., 2014). A few fully spliced (FS) and AS versions of *R* transcripts are targets of miRNAs and nonsense-mediated mRNA decay (NMD; Zhai et al., 2011; Shivaprasad et al., 2012; Gloggnitzer et al., 2014; Zhang et al., 2016), indicating that *R* gene expression is also under posttranscriptional control in plants.

NMD is a translation-coupled mRNA surveillance process in eukaryotes that prevents mRNAs containing premature termination codons (PTCs) from being translated. PTC-containing transcripts can arise from mutations or AS, and NMD is usually triggered by the presence of a downstream splice junction or long 3′ untranslated region (UTR; Rebbapragada and Lykke-Andersen, 2009; Peccarelli and Kebaara, 2014). FS natural transcripts can also be subject to NMD by virtue of containing NMD-triggering characteristics such as one or more introns in the 3′UTR, long 3′UTRs, or upstream open reading frames (uORFs) encoding no fewer than 35 amino acids (Kertész et al., 2006; Kerényi et al., 2008; Nyikó et al., 2009; Kalyna et al., 2012; Le Hir et al., 2016).

The canonical NMD process occurs when a translating ribosome encounters a PTC and fails to properly terminate translation. This leads to the phosphorylation and activation of the core NMD factor UP-FRAMESHIFT1 (UPF1), a process promoted by the interaction of UPF1 with UPF2 and UPF3, which associate with a downstream exon-junction complex (EJC; Kim et al., 2001; Banihashemi et al., 2006; Schweingruber et al., 2013). In a transient wild tobacco (*Nicotiana benthamiana*) assay, NMD factor SUPPRESSOR FOR MORPHOLOGICAL DEFECTS OF GENITALIA7 (SMG7) bound to the phosphorylated C-terminal region of UPF1 for subsequent recruitment of the decapping and deadenylation complexes before the decay of the target mRNA (Mérai et al., 2013). A recent study provided evidence that the dephosphorylation of UPF1 involves an SMG7 function (Kesarwani et al., 2019). NMD is involved in flowering, Suc metabolism, and stress responses in plants (Yoine et al., 2006; Jeong et al., 2011; Rayson et al., 2012; Riehs-Kearnan et al., 2012; Shi et al., 2012; Garcia et al., 2014; Gloggnitzer et al., 2014; Filichkin et al., 2015; Sureshkumar et al., 2016).

The most noteworthy function of NMD is its participation in the regulation of plant immunity. A null mutation in *UPF1* or *UPF3* confers disease resistance via increased levels of salicylic acid (SA) and elevated expression of defense genes, but this mutation also causes seedling lethality and late flowering in Arabidopsis (*Arabidopsis thaliana*; Jeong et al., 2011; Rayson et al., 2012; Riehs-Kearnan et al., 2012; Shi et al., 2012). A subset of FS natural TIR-NBS-LRR (TNL)–type *R* gene transcripts carrying NMD-eliciting features accumulated with known AS-coupled NMD (AS-NMD) transcripts in both *smg7-1*, an NMD-compromised Arabidopsis mutant showing autoimmunity, and a wild-type plant infected with *Pseudomonas syringae* pv *tomato* DC3000 (*Pst*DC3000; Gloggnitzer et al., 2014). In addition, the autoimmune phenotype of *smg7-1* requiring RESISTANT TO *P. SYRINGAE*6 (RPS6) was suppressed by the simultaneous mutation of *PHYTOALEXIN DEFICIENT4* (*PAD4*) or *ENHANCED DISEASE SUSCEPTIBILITY1* (*EDS1*), which are important for TNL-dependent signaling (Gloggnitzer et al., 2014). These findings suggest that autoimmunity in NMD-compromised mutants results from the activation of TNL-type R-dependent immunity and that bacterial infection might immediately suppress the NMD machinery in Arabidopsis. However, the pathway and timing of the decrease in NMD efficiency during *Pseudomonas* infection are still unclear.

Here, we analyzed the architecture of *R* genes expressed in NMD-compromised Arabidopsis mutants and found that most *R* genes produce transcripts that are targets of NMD. The recognition of bacterial infection by PRRs leads to the accumulation of a group of TNL- and CC-NBS-LRR (CNL)–type transcripts by triggering the decay of UPF proteins through the ubiquitin-26S proteasome system (UPS). These findings demonstrate that the expression of a subset of *R* genes is controlled by NMD in the face of pathogen infection.

RESULTS

Simultaneous Mutation of *UPF1* and *UPF3* Causes Severe Autoimmune Responses

Arabidopsis mutants with a defect in any of the genes encoding NMD core components (e.g., UPF1, UPF3, and SMG7) accumulate NMD-sensitive transcripts and exhibit autoimmunity and developmental arrest (Jeong et al., 2011; Drechsel et al., 2013; Gloggnitzer et al., 2014). When we performed reciprocal crosses of *upf1-5* and *upf3-1*, the resulting double mutants *upf1-5 upf3-1* and *upf3-1 upf1-5* exhibited distinctly dwarfed, curly leaves and seedling lethal phenotypes when grown under typical growth conditions (22°C, 16-h day/8-h night) but not when grown at a high temperature (28°C, 16-h day/8-h night; Figures 1A and 1B). When the plants were grown at 22°C under a 12-h day/12-h night photoperiod, the growth-arrested phenotypes were partially rescued in the double mutants (Supplemental Figure 1A). Thus, we used Arabidopsis plants grown under this neutral-day condition for pathophysiological studies.

To determine whether the simultaneous mutation of *UPF1* and *UPF3* would also reinforce resistance responses against bacterial infection, we analyzed the responses of wild-type, *upf1-5*, *upf3-1*, *upf1-5 upf3-1*, and *upf3-1 upf1-5* plants to infection with *Pst*DC3000 and *Pseudomonas cannabina* pv *alisalensis* ES4326 (*Pca*ES4326; formerly *P. syringae* pv *maculicola* ES4326; Bull et al., 2010). Although the number of bacteria in *upf1-5 upf3-1* and *upf3-1 upf1-5* leaves was comparable to that in *upf1-5* and *upf3-1*, these double mutants, but not any single mutant, exhibited severe necrotic symptoms 3 d after *Pseudomonas* infection (Figure 1C). Considering the atypical symptom development observed in *upf1-5 upf3-1* and *upf3-1 upf1-5* after virulent *Pseudomonas* infection, we tested whether basal defense responses are boosted in these double mutants after infection. The expression of *FLG22-INDUCED RECEPTOR-LIKE KINASE1*, *NDR1-HIN1-LIKE10* (MAMP-responsive genes), and *PATHOGENESIS-RELATED PROTEIN1* (*PR1*) was not significantly altered in the double mutants after *Pst*DC3000 infection compared with the single mutant or wild-type plants (Supplemental Figures 1B and 1C). Before infection, however, the expression levels of these genes were higher in the *upf3-1 upf1-5* mutant than in the other plants. These results suggest that immune-related genes are positively regulated in the double mutant. In addition, accelerated SA accumulation was observed in the double mutant both before and after *Pst*DC3000 infection (Supplemental Figure 1C).

Next, we examined the level of electrolytic leakage in Arabidopsis leaves after *Pst*DC3000 infection. Electrolyte leakage was more severe in the leaf disks of *upf3-1 upf1-5* than in the wild type, *upf1-5*, and *upf3-1* grown at 22°C during infection, while the level in every single mutant was not significantly different from that of wild-type plants (Supplemental Figure 1D, left representation).
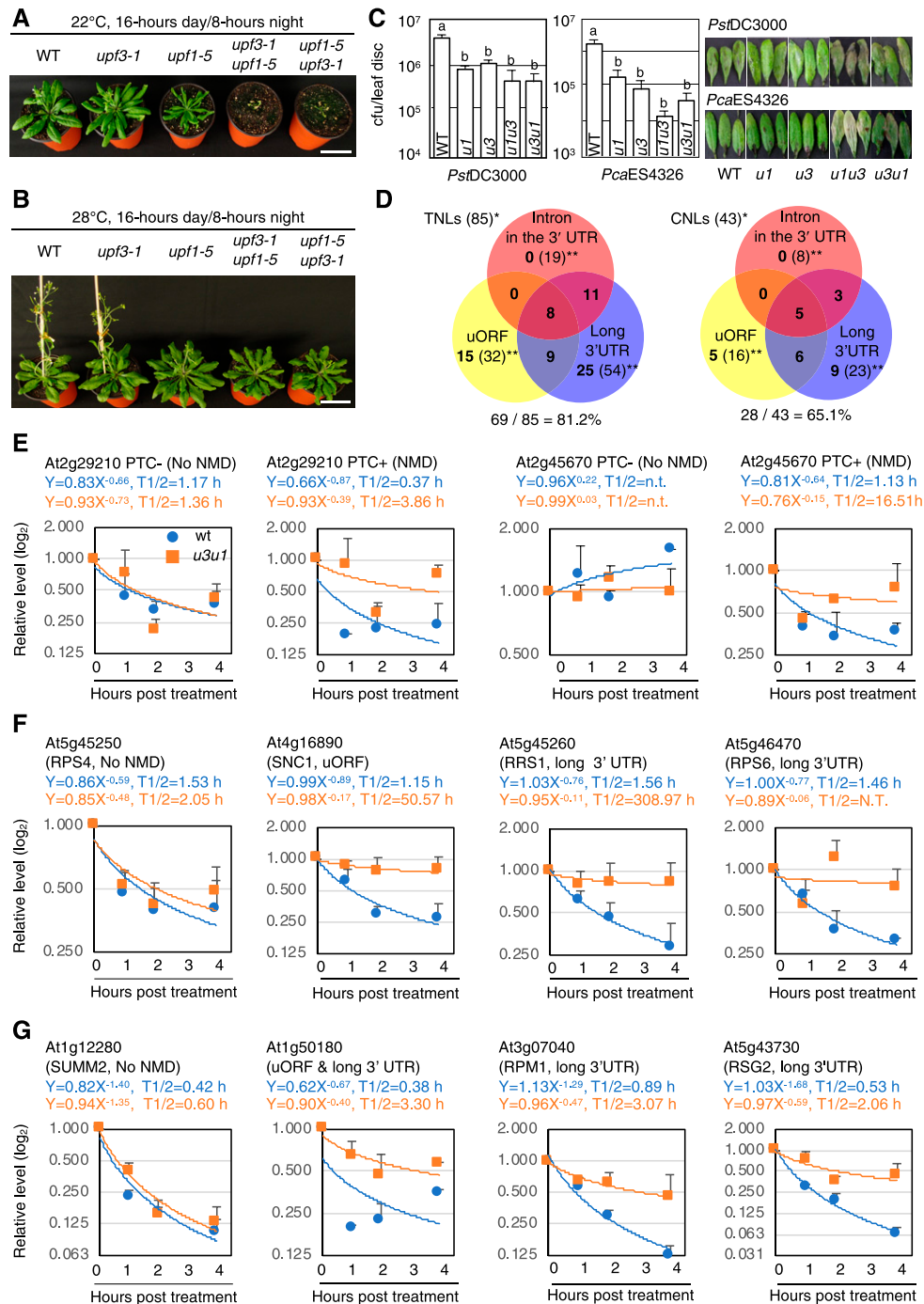
Figure 1. The *upf1 upf3* Double Mutants Exhibit Intensified Autoimmunity.

(A) and **(B)** Five-week–old Arabidopsis ecotype Columbia-0 (wild type [WT]), *upf1-5*, *upf3-1*, *upf1-5 upf3-1*, and *upf3-1 upf1-5* plants were grown at 22 ± 1°C **(A)** or 28 ± 1°C **(B)** with a 16-h d/8-h night photoperiod. Simultaneous mutation of *UPF1* and *UPF3* arrested Arabidopsis growth at 22°C, while the growth defect was moderately recovered by a temperature shift to 28°C. Scale bars = 5 cm.

(C) Bacterial counts and disease symptoms in the wild type (WT) and NMD-compromised mutants 3 d after *Pst*DC3000 and *Pca*ES4326 infection. Different letters (a and b) indicate statistically significant differences. P < 0.01; one-way ANOVA. Error bars indicate sᴇ (*n* = 8).

(D) Venn diagrams of TNL- and CNL-type *R* genes illustrating the number of genes carrying different NMD features. Numbers in parentheses are the total number of expressed genes (*) and the total number of genes bearing each NMD event (**).

(E) to **(G)** Stability of NMD reporters **(E),** representative TNL transcripts **(F)**, and representative CNL transcripts **(G)**. RT-qPCR analysis was performed using total RNA extracted from ActD-treated leaves of the wild type (WT) and *upf3-1 upf1-5* (*u3u1*) mutants that had been collected at 0, 1, 2, and 4 hpt. The

However, an increase in electrolyte leakage was not observed in the double mutant grown at 28°C (Supplemental Figure 1D, right representation). The transcripts of 39 TNL-type *R* genes were more stable in *smg7 pad4* than in *pad4*, 20 of which showed NMD-sensitive features (Gloggnitzer et al., 2014). To determine whether the accumulation of TNLs is a representative physiological characteristic in these *upf* mutants, we measured the mRNA levels of selected TNLs in plants under both NMD-compromised conditions (*upf1-5*, *upf3-1*, *upf1-5 upf3-1*, *upf3-1 upf1-5*, and cycloheximide [CHX]-treated wild type) and wild-type plants grown at two different temperatures. We analyzed well-characterized FS *R* gene transcripts showing NMD sensitivity (Gloggnitzer et al., 2014). We treated wild-type and mutant plants with actinomycin D (ActD) for 4 h to inhibit transcriptional elongation (Sobell, 1985), as described in a previous analysis of *upf3-1*, in which the 4-h treatment was found to be optimal without damaging plant tissues (Hori and Watanabe, 2005). This blockage of de novo transcription enables the NMD sensitivity of individual transcripts to be evaluated at the post-transcriptional level (Kurosaki et al., 2014). The known NMD-sensitive TNL transcripts (Gloggnitzer et al., 2014) accumulated under potent NMD-compromised conditions (in the double mutants and CHX-treated wild-type plants) regardless of temperature (Supplemental Figure 2). These results suggest that double mutants possessing an excessive amount of TNL transcripts remain under the control of temperature-dependent EDS1-mediated immune responses, as described for *smg7-1* (Wang et al., 2009; Alcázar and Parker, 2011; Heidrich et al., 2013; Carstens et al., 2014; Gloggnitzer et al., 2014; Stuttmann et al., 2016). Notably, the differences in transcript levels among the wild type and *upf* mutants were reduced when de novo transcription continued to occur compared with ActD-treated plants (DMSO in Supplemental Figure 2), indicating that continuous transcription is necessary for maintaining a steady-state level of *R* gene transcripts in Arabidopsis (Drechsel et al., 2013). Altogether, we propose that the accumulation of a variety of NMD-sensitive *R* transcripts leads to enhanced basal immunity in these mutants.

A Significant Number of *R* Gene Transcripts Retain NMD-Sensitive Characteristics

To comprehensively examine the extent to which the expressed *R* transcripts differ both quantitatively and qualitatively across wild-type and single– and double–mutant plants, we analyzed the FS natural transcripts and the AS variants of TNLs and CNLs based on our RNA-sequencing (RNA-seq) data of ActD-treated plants (Supplemental Data Set 1) and determined whether each transcript carried NMD-eliciting features (Supplemental Data Set 2; Supplemental Files 1 to 7). Among the 85 TNL and 43 CNL genes expressed, 19 and 8 of the TNL (22.3%) and CNL genes (18.6%) analyzed, respectively, contained at least one intron in the 3′UTR.

A long 3′UTR was the most common NMD feature of the FS *R* transcripts (63.5%, 54 TNLs out of 85; 53.4%, 23 out of 43 CNLs), ranging from 350 to 3,180 nucleotides in length. Thirty-two TNLs (37.6%) and 16 CNLs (37.2%) carried uORFs that either overlapped with the main ORFs or encoded peptides composed of no fewer than 35 amino acids (Table 1). In summary, the FS natural transcripts of 69 TNLs (81.2%) and 28 CNLs (65.1%) retained at least one of the three NMD-sensitive features (Figure 1D; Supplemental Data Set 2; Supplemental Files 6 and 7). The FS natural transcripts of 16 TNL and 15 CNL genes carried no NMD signals, but a range of their splicing variants (12 TNLs and 5 CNLs) were targets of AS-NMD (Table 1; Supplemental Data Set 2). Overall, 81 TNLs (95.3%) and 33 CNLs (76.7%) are potential NMD substrates. Previously, in Arabidopsis studies, 1 to 2% of the natural transcripts and 13 to 17.4% of intron-containing genes were shown to be upregulated in NMD-deficient plants (Yoine et al., 2006; Kurihara et al., 2009; Kalyna et al., 2012; Drechsel et al., 2013), demonstrating that plant *R* genes are highly enriched in NMD regulation.

Next, we tested the stability of these NMD-susceptible FS *R* transcripts in *upf3-1 upf1-5* mutants by measuring the half-lives of *R* transcripts from leaf samples taken from wild-type and mutant plants at 0, 1, 2, and 4 h after blocking de novo transcription. We used *At2g29210* and *LYSOPHOSPHATIDYLETHANOLAMINE ACYLTRANSFERASE2* (*LPEAT2*) AS variants (PTC+) as NMD controls (Gloggnitzer et al. 2014). The half-lives of these NMD markers and *R* transcripts carrying the NMD-sensitive features were elevated in *upf3-1 upf1-5* compared with normal-looking transcripts showing similar levels of stability between wild type and *upf3-1 upf1-5* (Figures 1E to 1G; Supplemental Figure 3), indicating that NMD is one of the main processes controlling the expression of TNL and CNL genes. Other transcripts bearing NMD-sensitive features, however, showed no differences in RNA stability between wild type and *upf3-1 upf1-5*, e.g., *RPP5* (Supplemental Figure 3). This result suggests that not all *R* genes bearing NMD-sensitive features are genuine NMD targets, as widely observed in eukaryotic genes (Rebbapragada and Lykke-Andersen, 2009; Kurosaki et al., 2014; Peccarelli and Kebaara, 2014).

To determine whether FS natural TNL and CNL transcripts are post-transcriptionally regulated, we measured the transcription rates of the randomly selected genes by performing a chromatin immunoprecipitation (ChIP) assay of wild-type and *upf3-1 upf1-5* plants using an α-RNA polymerase II (α-RNAPII) C-terminal domain antibody, and primer sets specific to regions between the transcription and translation initiation sites. The ChIP signals in the TNL genes were largely constant between the wild type and *upf3-1 upf1-5* (Supplemental Figure 4A), indicating that most TNL-type *R* genes with NMD-sensitive features are constitutively transcribed in Arabidopsis leaves and that the resulting transcripts are subject to immediate turnover by NMD in the wild type. Unlike TNLs, half of

Figure 1. (continued).

half-lives were calculated by nonlinear least-squares regression analysis (average ± SD, *n* = 3; three biological replicates with three technical repeats). Stability analyses of other *R* transcripts are provided in Supplemental Figure 3. Sequences of the individual primers used in this study are presented in Supplemental Data Set 3.

Table 1. Detailed NMD-Sensitive Characteristics of 85 TNL and 43 CNL Genes Expressed in Arabidopsis Leaves

		Number of Genes (%)	
		TNLs	CNLs
NMD-Sensitive Features	Intron in the 3′ UTR	19 (22.3%)	8 (18.6%)
	Long 3′ UTR	54 (63.5%)	23 (53.4%)
	uORF	32 (37.6%)	16 (37.2%)
AS-NMD		43 (50.6%)	13 (30.2%)
Alternative promoters to NMD		12 (27.9%)	7 (16.3%)
Alternative polyadenylation to NMD		15 (17.6%)	3 (7.0%)
Fusion transcripts between the flanking genes resulting in NMD		9 (10.6%)	7 (16.3%)

the CNL genes tested here showed higher enrichment of the RNAPII elongation complex in *upf3-1 upf1-5* than in wild type, e.g., *RPP7* and *RPM1* (Supplemental Figure 4B), suggesting that these genes are transcriptionally upregulated in the *upf3-1 upf1-5* mutant. Taken together, these findings support the notion that NMD is one of the regulatory pathways controlling the steady-state levels of both FS and AS *R* transcripts carrying NMD-sensitive features (Gloggnitzer et al., 2014).

Bacterial Infection Results in Turnover of UPF Proteins

Because bacterial infection upregulates a subset of NMD-sensitive transcripts (Gloggnitzer et al., 2014), we monitored the transcript levels of core NMD factors in *Pst*DC3000-infected wild-type leaves to detect any decrease in transcript levels upon bacterial infection. The FS natural transcripts encoding Arabidopsis UPF1, UPF3, and SMG7 are known NMD substrates (Nyikó et al., 2013; Gloggnitzer et al., 2014; Degtiar et al., 2015; Kesarwani et al., 2019). Our RNA-seq data also revealed that the *UPF1* transcript, a possible NMD target, carries a 508 nucleotides–long 3′UTR (Supplemental Figure 5A). These transcripts were upregulated after *Pst*DC3000 infection, while the level of the FS *UPF2* transcript remained constant (Supplemental Figure 5A). The upper products, which accumulated during infection, were identified as variants of *UPF1* and *UPF2* produced by unspliced introns 26 and 14, respectively, and they eventually retained NMD-triggering features owing to the long 3′UTR containing two introns (single and double asterisks, Supplemental Figures 5A and 5B). The results indicate that the plant NMD system becomes impaired at an early stage of infection, despite the increasing levels of transcripts of NMD factors (Kerényi et al., 2008; Nyikó et al., 2013; Gloggnitzer et al., 2014; Degtiar et al., 2015; Shaul, 2015).

The inconsistency between the increased transcript levels of *UPF* genes and the reduction in NMD activity after infection (Gloggnitzer et al., 2014) suggests that bacterial infection might disrupt the plant NMD system by affecting the integrity of the machinery at the protein level. To address this hypothesis, we prepared monoclonal antibodies against UPF1 (α-UPF1), UPF2, and UPF3 and used them for immunoblot analysis (Supplemental Figures 6B and 6C). α-UPF1 detected a faint signal of UPF1 in the knockdown mutant *upf1-5* and in the putative knockdown mutant *upf1-4*. However, the protein was undetectable in the amino acid substitution mutant *upf1-1* for unknown reasons (Supplemental Figure 6B). We examined the levels of UPF1, UPF2, and UPF3 in wild-type leaves infected with *Pst*DC3000 using α-UPF1, α-UPF2,

and α-UPF3. The levels of UPF1 and UPF3 were reduced to <40% (UPF1) to 50% (UPF3) within 0.5 h post inoculation (hpi) and became undetectable from 10 to 30 hpi, whereas the level of UPF2 was maintained for up to 6 hpi. All three NMD factors were undetectable by 20 hpi (Figure 2A). The turnover of UPF1 occurred more quickly than that of UPF3, i.e., UPF3 was still detectable at 10 hpi when UPF1 was absent (Figure 2A, upper representation).

Because UPF1 decay began as early as 30 min post inoculation (mpi; Figure 2A, upper representation), we wondered how early the turnover of UPF proteins was initiated. We monitored the stability of UPF proteins at various time points beginning at 1 mpi with *Pst*DC3000. Surprisingly, the reduction in UPF1 levels was clearly observed at 5 mpi, and a sharp decrease occurred between 15 and 20 mpi, after which only ~50% UPF1 remained. A drastic decrease in UPF3 levels was observed between 15 and 25 mpi, during which >90% of UPF2 remained (Figure 2A, lower representation). These findings suggest that the turnover of UPF proteins is an early response to *Pst*DC3000 infection.

To determine whether other protein components involved in NMD (Kerényi et al., 2008) are also unstable upon bacterial infection, we generated transgenic Arabidopsis plants over-expressing the SMG7 and EJC proteins. SMG7 and the other EJC components—Y14, MAGO, eIF4AIII, and CASC3/Barentsz (BTZs)—were stably maintained during infection compared with the overexpressed UPF proteins, although the overexpressed versions of UPF proteins (the first to third rows of the left representation in Figure 2B) were destabilized later than the native proteins (Figure 2B). Thus, we conclude that bacterial infection initiates the specific destruction of UPF proteins.

To determine whether the decay of UPF proteins is initiated by only virulent *Pseudomonas* infection, we inoculated wild-type plants with an attenuated strain, *Pst*DC3000 *hrcC⁻*, and two avirulent derivatives of *Pst*DC3000 carrying *AvrRpm1* or *AvrRps4* and subjected them to immunoblot analysis using an anti-UPF1 polyclonal antibody. Like the turnover pattern of UPF1 in *Pst*DC3000-infected plants, infection with these different strains also triggered the decay of UPF1 proteins in Arabidopsis (Supplemental Figures 7A and 7B), indicating that the sensing of *P. syringae* is sufficient to initiate the decay of the core NMD factors. Unlike the immunoblotting results obtained using monoclonal α-UPF1 antibody, the UPF1 level at 6 hpi was somehow recovered, which was more pronounced after infection with the *Pst*DC3000 *hrcC⁻* strain. Furthermore, a putative UPF1 degradation product (single asterisk in Supplemental Figure 7) was also observed in parallel with UPF1 dynamics and was not detected in
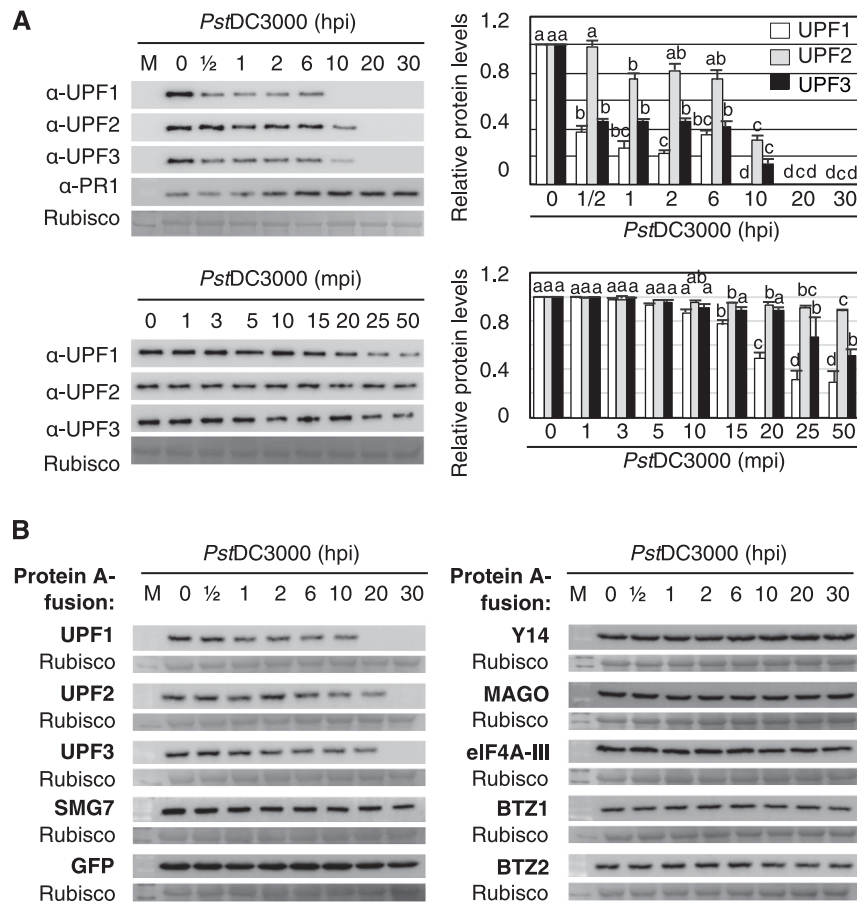
Figure 2. UPF1, UPF2, and UPF3 Decay during an Early Phase of *Pst*DC3000 Infection.

(A) Dynamics of UPF1, UPF2, and UPF3 proteins up to 30 hpi (top) and 50 mpi (bottom). Immunoblot analyses (left) were performed for leaf samples taken from wild-type Col-0 plants that had been infected with *Pseudomonas* and collected at the indicated time points using an anti-UPF1 monoclonal antibody (α-UPF1), α-UPF2, or α-UPF3. The right shows UPF protein levels in infected leaves at the indicated time points (average $\pm$ SD, $n = 4$). Different letters above the bars (i.e., a, b, c, d, ab, and bc) indicate statistically significant differences (P < 0.05, one-way ANOVA). Successful infection was verified by examining the levels of PR1. Both experiments were performed with four biological replicates.
(B) The NMD factor SMG7 and the EJC core protein components, but not UPF1, UPF2, or UPF3, remained stable during *Pst*DC3000 infection. The leaves of transgenic Arabidopsis plants (T$_3$) stably expressing protein A-fused UPF1, UPF2, UPF3, SMG7, Y14, MAGO, eIF4A-III, BTZ1, and BTZ2 were infected with *Pst*DC3000 and collected at the indicated time points after infection for immunoblot analysis. GFP-protein A was used as a representative stable protein. The recombinant proteins were detected using an α-PAP antibody. M, prestained protein ladder.

the blots using monoclonal α-UPF1 antibody. We speculate that UPF1 might undergo a conformational change during the decay process and that the monoclonal antibody is unable to cross react with this transitional form of UPF1. The detection of a small product by the polyclonal antibody even before infection (single asterisk in Supplemental Figure 7) suggests that the UPF1 level may be controlled posttranslationally under normal conditions.

UPF1 and UPF3 Are Destroyed Via Ubiquitination at an Early Stage of Infection

To examine whether UPF proteins are post-translationally degraded during an early stage of infection, MG132, an inhibitor of the proteasome, was coinfiltrated into wild-type Arabidopsis leaves with *Pst*DC3000. While the coapplication of the solvent

DMSO alone with *Pst*DC3000 did not affect the protein dynamics of UPF1, UPF2, or UPF3, MG132 coinfiltrated with *Pst*DC3000 interrupted the infection-induced destruction of these proteins (Figure 3A). These results support our observation that the reduction and subsequent disappearance of UPF proteins resulting from *Pseudomonas* infection (Figure 2) is due to the decay of UPF proteins rather than the translational inhibition of mRNAs encoding these NMD factors.

To confirm that the decay of the UPF proteins occurs via the UPS during bacterial infection, we monitored the levels of ubiquitinated UPF proteins in the α-UPF1, α-UPF2, and α-UPF3 immunoprecipitates by immunoblot analysis using an α-ubiquitin (α-UBQ) antibody. The ubiquitination of UPF1 and UPF3 was strongly induced at 30 mpi and 1 hpi, respectively (Figure 3B; Supplemental Figure 8A), which is consistent with the dynamics of these proteins
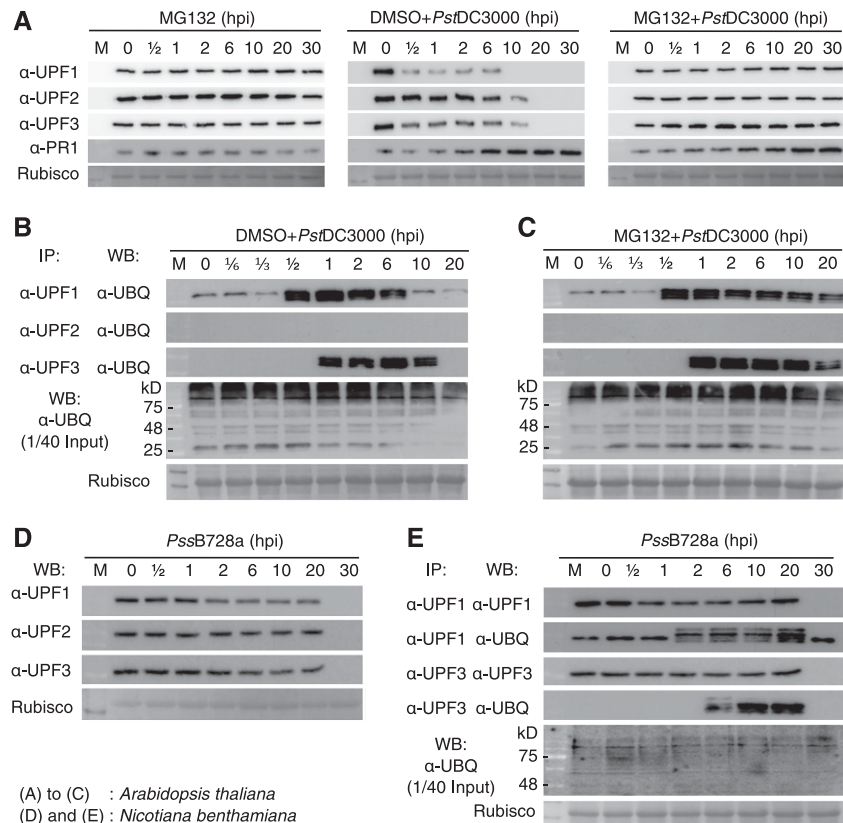
Figure 3. *P. syringae* Infection Induces Ubiquitination of UPF1 and UPF3 in Arabidopsis and *N. benthamiana* Plants.

(A) Effects of the 26S proteasome inhibitor MG132 on the decay of UPF1, UPF2, and UPF3 during infection. DMSO alone or MG132 dissolved in DMSO was coinfiltrated into wild-type leaves with *Pst*DC3000. Immunoblot analyses were performed using α-UPF1, α-UPF2, or α-UPF3. Successful infection was verified by examining the levels of PR1.

(B) Ubiquitination of UPF1 and UPF3, but not UPF2, in wild-type leaves after *Pst*DC3000 infection. Immunocomplexes with the α-UPF1, α-UPF2, or α-UPF3 antibody were subjected to immunoblotting with α-UBQ.

(C) IP assay with proteins extracted from MG132+*Pst*DC3000-treated wild-type plants. The levels of UPF proteins in IP complexes in **(B)** and **(C)** are shown in Supplemental Figure 8A and 8B, respectively.

(D) Degradation of UPF proteins in *N. benthamiana* leaves infected with *P. syringae* pv *syringae* B728a (*Pss*B728a).

(E) Induction of UPF1 and UPF3 ubiquitination in *N. benthamiana* leaves during *Pss*B728a infection. Levels of ubiquitinated UPF1 and UPF3 were determined by IP with α-UPF1 or α-UPF3 and subsequent immunoblot analysis with α-UPF1, α-UPF3, and α-UBQ.

(Figure 2A). These results suggest that the ubiquitination of UPF1 and UPF3 is a temporally controlled early response in plant immunity. UPF1 was already ubiquitinated before infection (Figure 3B), which likely explains the previous findings that the turnover of UPF1 occurs within 4 h in ActD-treated *upf1-5* plants (Supplemental Figure 6C) and that the putative degradation product was detected by polyclonal α-UPF1 antibody even before infection (single asterisks in Supplemental Figure 7). These results suggest that, in Arabidopsis, UPF1 levels are also regulated by ubiquitination under normal growth conditions. The induced ubiquitination signals of UPF1 and UPF3 were maintained for up to 6 and 10 hpi (Figure 3B), respectively, when the proteins were still present (Figure 2A). The ubiquitinated UPF1 and UPF3 signals, however, were no longer evident at 10 hpi and 20 hpi, respectively, and at 20 hpi, both were nearly or entirely undetectable (Figure 3B), indicating that the induction of UPF1/UPF3 ubiquitination is responsible for the decay of these proteins. To validate this result,

we treated plants with MG132 and *Pst*DC3000 infection and found that the induced level of UPF1 and UPF3 ubiquitination signals was maintained through 20 hpi (Figure 3C; Supplemental Figure 8B), supporting the suggestion from Figure 3B that the disappearance of the induced ubiquitination signals was due to the absence of both proteins at this stage. We did not detect multiple bands larger than UPF1 and UPF3 (estimated molecular masses of 136.9 and 54.0 kD, respectively), suggesting that these proteins are degraded by the 26S proteasome via mono-ubiquitination or multi-monoubiquitination rather than poly-ubiquitination (Shabek et al., 2012; Ciechanover and Stanhill, 2014; Braten et al., 2016).

UPF2, which is also decayed during *Pst*DC3000 infection (Figures 2A and 3A), was not ubiquitinated after infection (Figures 3B and 3C). Because UPF2 and UPF3 are present in complexes from the nucleolus to the cytoplasm (Kerényi et al., 2008; Kim et al., 2009), we reasoned that UPF2 might enter the 26S proteasome

complex with UPF3 during infection. Indeed, UPF2 coimmuno-precipitated with UPF3 under both uninfected and *Pst*DC3000-infected conditions (Supplemental Figure 9). To test whether UPF1/UPF3 decay upon bacterial challenge is universal among plants, we subjected *N. benthamiana* plants to infection with the known bacterial pathogen *P. syringae* pv *syringae* B728a (*Pss*B728a). The UPF proteins of the *N. benthamiana* plants were also destroyed by 30 hpi (Figure 3D). The induction of UPF1 and UPF3 ubiquitination was detected at 2 and 6 hpi, respectively (Figure 3E), suggesting that plant immunity involves the suppression of NMD via the control of UPF protein levels in members of the *Solanaceae* family.

Because TNL genes are known to be deregulated upon *Pseudomonas* infection due to decreased NMD efficiency (Gloggnitzer et al., 2014), we investigated whether the kinetics of the NMD-sensitive TNL and CNL transcripts reflect the decay of UPF proteins upon *Pst*DC3000 infection. We monitored the stability of TNL and CNL transcripts from ActD-treated infected leaves taken at 0, 1, 2, and 4 hpi by RT-qPCR analysis. The transcripts of NMD markers as controls, namely, *At2g29210* and *LPEAT2* retaining PTC (*At2g29210* PTC+ and *LPEAT2* PTC+), were more stably maintained in infected wild-type leaves than in noninfected leaves (Figure 4A). Similarly, the TNL and CNL transcripts bearing NMD-sensitive features, e.g., *SIKIC3*, *RPS6*, *RPM1*, and *RPP7*, were more long-lived in infected leaves than in noninfected leaves (Figures 4B and 4C; Supplemental Figure 10). The half-lives of *SNC1* and *RPP5*, which are representative targets of small-interfering RNA (Yi and Richards, 2007), and non-NMD targets, namely, *SUMM2* and *RPS4*, were similar between infected and noninfected leaves (Figures 4B and 4C; Supplemental Figure 10). The gaps between the NMD target *R* transcripts in infected and noninfected plants were less distinct than those between *upf3-1 upf1-5* and wild type (Figures 1F, 1G, 4B, and C4C; Supplemental Figures 3 and 10), suggesting that NMD may have still occurred by 4 hpi, when UPF1 is still present (Figures 2A and 3B).

In parallel, we analyzed the accumulation of *R* transcripts in infected leaf samples taken at the same time points (Figures 2 and 3) used for protein analysis. As a result, we were able to sort the *R* genes bearing NMD-sensitive features into three groups. The early-response *R* genes, including *RPM1* and *At3g44400*, were upregulated as early as 30 mpi of *Pst*DC3000 (Figure 4; Supplemental Figure 11), suggesting that the transcripts of these genes are instantly stabilized when the UPF1 level is reduced to <40%. The second group, the so-called late-response genes, e.g., *SOC3*, *At3g14470*, *At4g14610*, and *At5g38340*, appeared to be upregulated later than 10 hpi, when UPF1 is completely decayed (Supplemental Figure 10). The nonresponsive genes, including *RRS1* and *At5g35450*, were not regulated by *Pseudomonas* infection (Supplemental Figure 10).

The miRNA target CNL-type *R* genes *At1g50180* and *RSG2* (Boccara et al., 2015; Cai et al. 2018), carrying uORF/long 3′UTR and long 3′UTR, respectively, are thought to also be targets of NMD, because their transcripts are stabilized upon *Pseudomonas* infection (Supplemental Figure 10B). By contrast, the half-lives of other known miRNA targets including *RPS5*, *At1g12290,* and *At1g61180* were not altered or shortened by the mutation of *UPF1/UPF3* or *Pseudomonas* infection (Supplemental Figure 11A),

suggesting that the steady-state level of a subset of CNL transcripts bearing NMD-sensitive features may be under the control of miRNA-mediated gene silencing rather than NMD. Moreover, three TNL-type *R* transcripts, *At3g44400*, *At4g14370*, and *At5g41740*, which were upregulated as early as 30 mpi by *Pseudomonas* infection, were more stable in infected versus noninfected plants. By contrast, the stability of these transcripts was reduced in *upf3-1 upf1-5* versus wild-type plants (Supplemental Figure 11B). These results suggest that susceptibility to NMD varies across FS *R* transcripts carrying NMD-sensitive features (Rebbapragada and Lykke-Andersen, 2009; Kurosaki et al., 2014; Peccarelli and Kebaara, 2014) and that the control of the expression of these genes might involve other processes, e.g., transcriptional regulation, under a variety of conditions. Based on these results, we propose that NMD is one of the main posttranscriptional control pathways involved in maintaining *R* transcript levels in Arabidopsis during the immunity response.

The Induction of UPF3 Ubiquitination Partially Depends on UPF1

The Cys- and His-rich domain of UPF1, which serves as a Really Interesting New Gene-related E3 ligase, is responsible for the UPF3-dependent self-ubiquitination required for activation of NMD in yeast (Takahashi et al., 2008). To determine whether UPF3 is required for UPF1 ubiquitination and vice versa in Arabidopsis, we monitored the ubiquitination and turnover of UPF proteins in *upf1-1*, *upf2-12*, and *upf3-1* plants at 1 h after *Pst*DC3000 infection. The ubiquitination level of UPF1 was similar across the wild type, *upf2-12*, and *upf3-1* (Figure 5A; second row in Figure 5B), suggesting that the induction of UPF1 ubiquitination upon *Pst*DC3000 infection occurs independently of UPF2 or UPF3. By contrast, the level of ubiquitinated UPF3 decreased 1.24 ± 0.042-fold in *upf1-1* compared with the wild type (fourth row in Figure 5B; sixth row in Figure 5C). The UPF3 level stabilized from 1 to 10 hpi in *upf1-1* compared with wild type (third and sixth rows in Figure 5C), most likely due to decreased ubiquitination. These results are consistent with the observation that the decay of UPF1 occurs before that of UPF3 (Figures 2A and 3B and 3C), and that UPF1 protein itself or ubiquitinated UPF1 modulates the ubiquitination of UPF3 upon bacterial infection. Bacterial infection induces the ubiquitination of UPF1/UPF3 for the decay of three UPF proteins, which differs from the UPF3-dependent self-ubiquitination of UPF1 required for NMD in yeast (Takahashi et al., 2008).

Microbial Perception by PRRs Initiates the Decay of UPF Proteins

NMD-sensitive transcript levels also increased in wild-type plants treated with 1 µM of the bacterial elicitor flg22, while the expression of these transcripts was suppressed in *flagellin sensitive2* (*fls2*) mutants (Gloggnitzer et al., 2014), suggesting that MAMP recognition can also affect the integrity of UPF proteins. Compared with mock treatment, in which the levels of UPF proteins were unchanged, both UPF1 and UPF3 started to degrade at 1 and 2 h post treatment (hpt) with flg22 in wild-type plants, respectively,
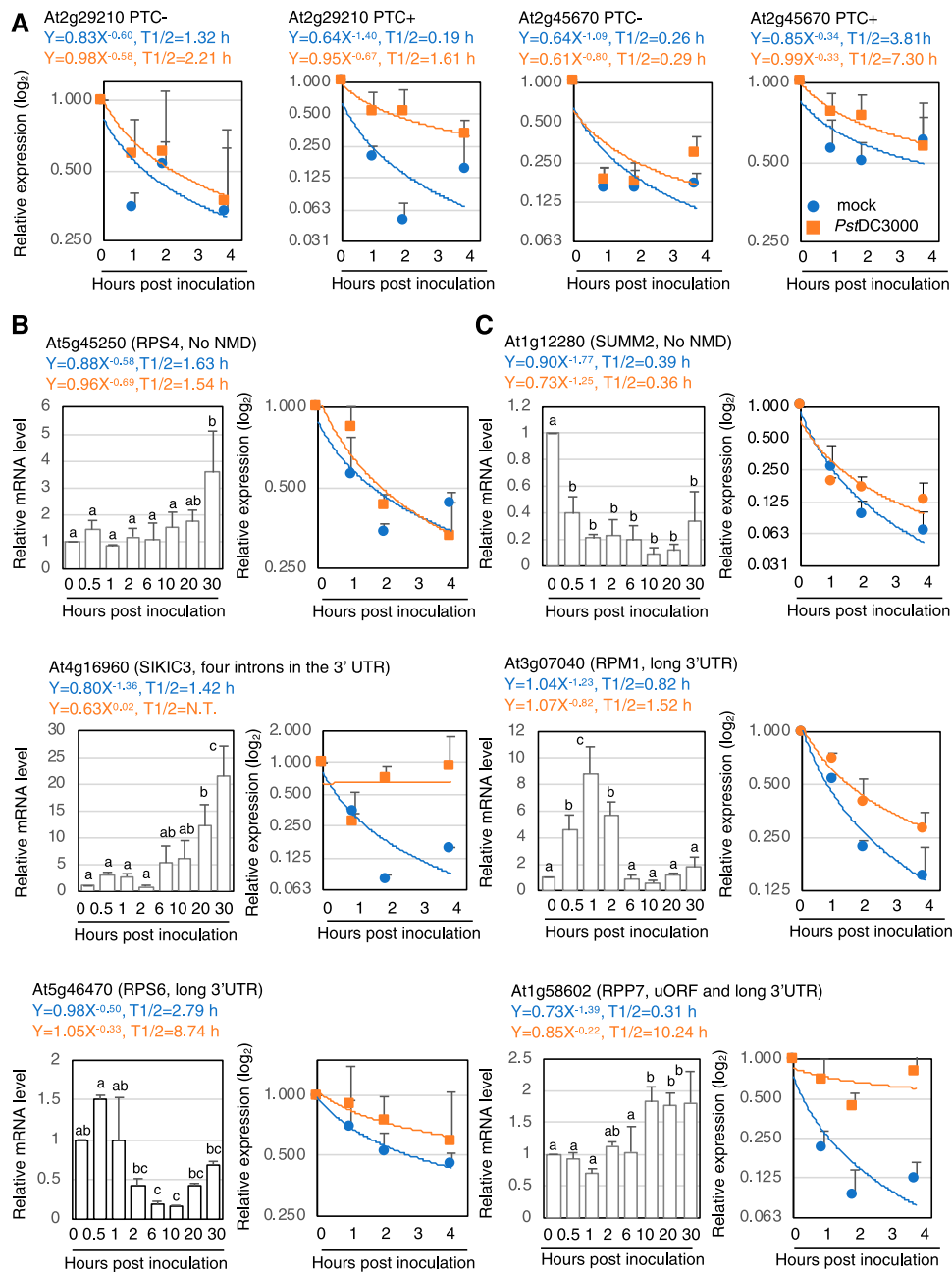
Figure 4. Steady-State Levels and the Stability of *R* Transcripts in *Pst*DC3000-Infected Wild-Type Plants.

(A) Stability of NMD markers *At2g29210* PTC+ and *LPEAT2* PTC+ in infected wild-type leaves.

(B) and **(C)** Transcript levels and half-lives of representative TNL transcripts, the non-NMD target *RPS4*, and *SIKIC3* and *RPS6* bearing NMD-sensitive features **(B)**, and CNL transcripts, the non-NMD target *SUMM2*, and the NMD-targets *RPM1* and *RPP7* **(C)**. Left, steady-state levels of selected *R* transcripts were measured in infected wild-type leaves during *Pst*DC3000 infection without ActD treatment. Data points are the average $\pm$ SD of three biological replicates with two technical repeats ($n = 3$). Different letters (i.e., a, b, c, ab, and bc) above the bars indicate statistically significant differences (P < 0.01, one-way ANOVA). Right, either ActD alone (cyan) or ActD together with *Pst*DC3000 (magenta) was infiltrated into wild-type leaves, and the treated leaves were collected at the indicated time points. Data points are the average $\pm$ SD of three biological replicates with three technical repeats ($n = 3$). Sequences of the gene-specific primers are presented in Supplemental Data Set 3.
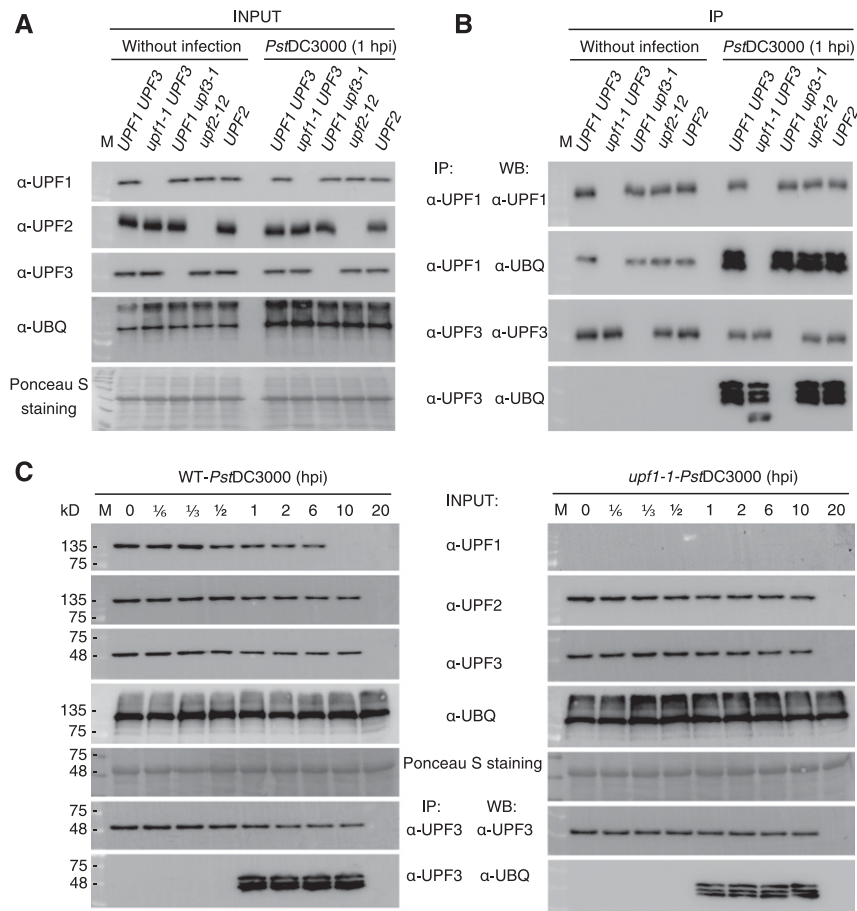
Figure 5. Induction of UPF1 Ubiquitination Occurs Independently of UPF2 or UPF3, While UPF1 Positively Affects the Induction of UPF3 Ubiquitination.

(A) Levels of UPF1, UPF2, and UPF3 in the leaves of the wild type (*UPF1 UPF3* and *UPF2*) and the mutant (*upf1-1 UPF3*, *UPF1 upf3-1*, and *upf2-12*) plants before and after *Pst*DC3000 infection (1 hpi). M, prestained protein ladder.

(B) Induction of UPF1 and UPF3 ubiquitination in wild-type and mutant plants. Protein complexes with the α-UPF1 or α-UPF3 antibody were subjected to immunoblot analyses with α-UBQ. Notably, depletion of UPF3 did not affect the induction of UPF1 ubiquitination (second row), while the induced ubiquitination signal of UPF3 was reduced in the *upf1-1* allele (fourth row). The experiment was performed with three biological replicates, which showed similar results. M, prestained protein ladder

(C) Depletion of UPF1 reduces the ubiquitination level of UPF3 during *Pst*DC3000 infection. Total proteins were extracted from the wild type (WT) and *upf1-1* that had been infected with *Pst*D3000 and immunoprecipitated with α-UPF3 to examine whether UPF3 is differentially ubiquitinated between the wild type and *upf1-1* mutant at the indicated time points. The immunocomplexes were subjected to immunoblotting with α-UPF3 or α-UBQ. M, prestained protein ladder.

while UPF2 levels were significantly reduced at 6 h (Figure 6A). flg22 treatment did not trigger the decay of UPF proteins in *fls2* or the co-receptor mutant *bri1-associated receptor kinase1-5* (*bak1-5*), although UPF1 in *bak1-5* disappeared within 30 h (Figure 6B). These findings suggest that the flg22-FLS2 association is pivotal for the effect of flg22 on UPF proteins. Consistent with UPF degradation via the UPS during *Pseudomonas* infection, flg22 treatment also caused the ubiquitination of UPF1 and UPF3 but not UPF2, and induced ubiquitination was observed at 1 and 2 hpt for UPF1 and UPF3, respectively (Figure 6C; Supplemental Figures 8C and 8D), when these proteins began to be destroyed (Figure 6A). Ubiquitination of UPF1 and UPF3 was uninducible in *fls2* or delayed to 20 hpt in *bak1-5* compared with 1 to 2 hpt in

wild-type plants (Figure 6D). These results indicate that the perception of MAMPs is sufficient for initiation of the ubiquitination of UPF1 and UPF3 during infection. The decay of UPFs was still triggered in *fls2* and *bak1-5* after *Pst*DC3000 infection, although the proteins were more stable in these mutants than in the wild type (Figure 6E). The relatively high dose of flg22 described above did not induce as strong a response in UPF proteins as *Pst*DC3000 infection (compare Figures 2A and 3B with Figures 6A and 6C, respectively). These findings suggest that microbial sensing by PRRs leads to the decay of UPF proteins, that other pathogen-derived molecules might simultaneously act during this early event, and that unidentified bacterial effectors might also contribute to the decay process.
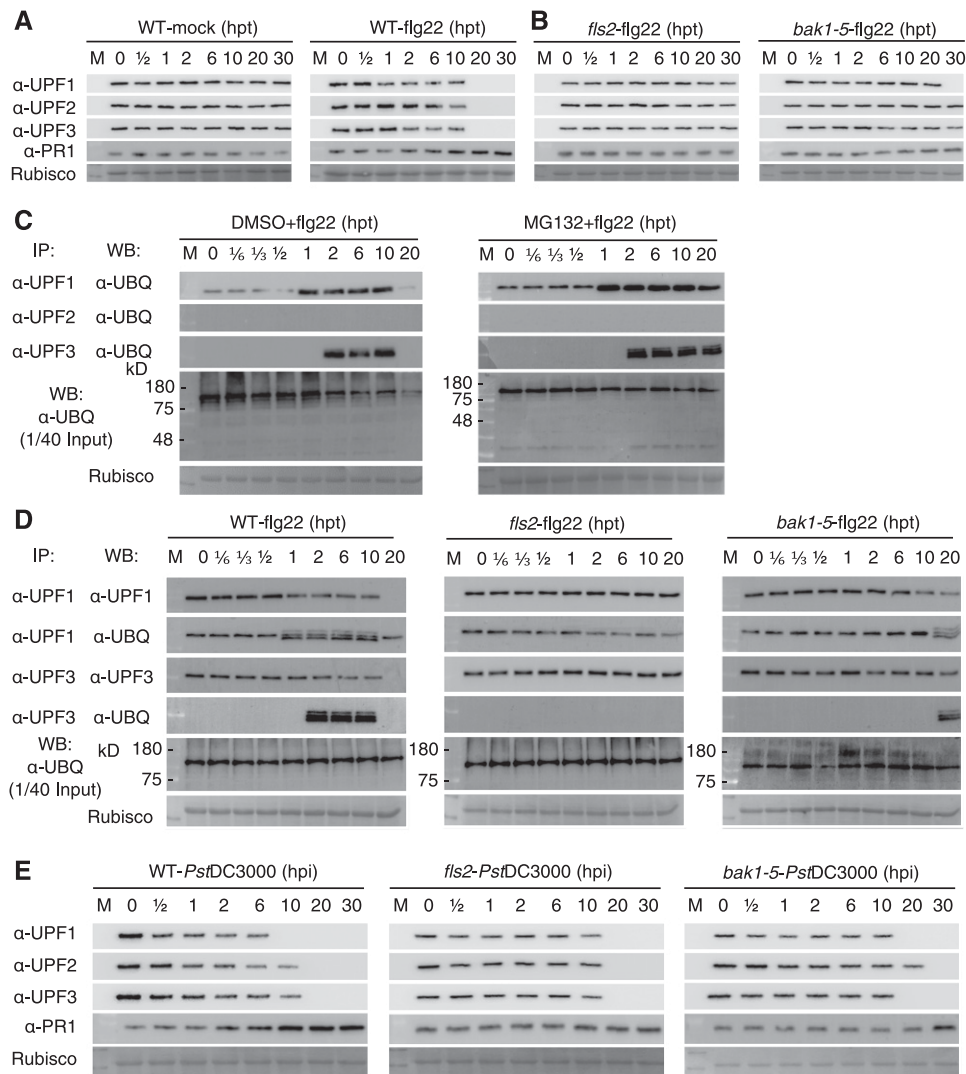
Figure 6. The Recognition of the Representative MAMP flg22 Is Sufficient To Trigger UPF Protein Decay in Arabidopsis.

(A) Dynamics of UPF1, UPF2, and UPF3 proteins in wild-type (WT) leaves treated with 10 mM of MgSO₄ (WT-mock) or 1 μM of flg22 (WT-flg22) up to 30 hpt. M, prestained protein ladder.

(B) The extracellular immune receptor (FLS2) and the coreceptor (BAK1) are required to initiate degradation of the UPF proteins upon flg22 treatment. M, prestained protein ladder.

(C) Perception of flg22 induces ubiquitination of UPF1 and UPF3 in wild-type (WT) leaves. Levels of the UPF proteins in the IP complexes are shown in Supplemental Figures 8C and 8D. M, prestained protein ladder.

(D) No or delayed induction of UPF1/UPF3 ubiquitination is observed after flg22 treatment in the *fls2* and *bak1-5* mutants, respectively. M, prestained protein ladder.

(E) Levels of UPF1, UPF2, and UPF3 proteins in wild-type (WT), *fls2*, and *bak1-5* leaves during *Pst*DC3000 infection. M, prestained protein ladder.

MITOGEN-ACTIVATED PROTEIN KINASE3 and MITOGEN-ACTIVATED PROTEIN KINASE6 Regulate the Induction of UPF1 and UPF3 Ubiquitination

The perception of microbial infection rapidly triggers an oxidative burst and dual phosphorylation of MITOGEN-ACTIVATED PROTEIN KINASE3 (MPK3) and MPK6 in plants (Nicaise et al., 2009). To examine whether the degradation of UPF proteins is associated with these early events, we observed the decay of these proteins

in wild-type and mutant plants defective in early signaling. UPF1 turnover occurred by 20 hpi after *Pst*DC3000 infection in *mpk3* and *mpk6* compared with 10 hpi in the wild type. UPF1 was still detectable until 20 hpt after flg22 treatment in *mpk6* cells (Figure 7A). To address whether the induction of UPF1/UPF3 ubiquitination is affected by mutations in *MPK3* and *MPK6*, we monitored the α-UPF1 and α-UPF3 immunoprecipitates from flg22-treated *mpk3* and *mpk6* leaves by immunoblotting using an α-UBQ antibody. The induction of UPF1 ubiquitination was initiated at 2 and
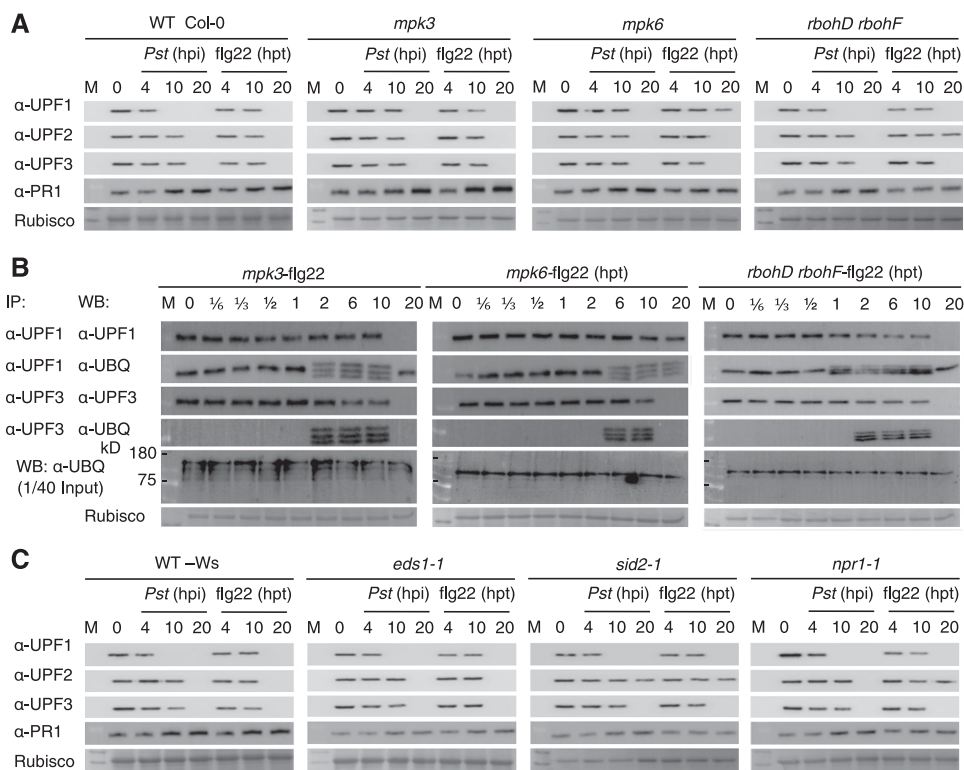
Figure 7. Initiation of UPF Protein Decay Involves a MAPK Pathway.

(A) Levels of UPF1, UPF2, and UPF3 in the leaves of *mpk3*, *mpk6* (defective in the MAPK cascade), and *rbohD rbohF* (defective in the ROS burst) mutants after recognition of flg22 and *Pst*DC3000 infection. M, prestained protein ladder; WT, wild type.

(B) MPK3 and MPK6, but not RBOHD or RBOHF, are genetically required for the induction of UPF1 and UPF3 ubiquitination. M, prestained protein ladder.

(C) *EDS1* (a key player in TNL-type R-triggered immunity and SA regulation), *ICS1/SID2* (SA biosynthesis), and *NPR1* (SA response) are dispensable for the decay of UPF1, UPF2, and UPF3. M, prestained protein ladder; WT, wild type.

Wild-type and mutant plants were either inoculated with *Pst*DC3000 or treated with 1 μM of flg22 and then used for immunoblotting. Col-0 is the parental line of *mpk3*, *mpk6*, *rbohD rbohF*, *sid2-1*, and *npr1-1*, while Wassilewskija (Ws) is the parental line of *eds1-1*.

6 hpt in *mpk3* and *mpk6*, respectively, compared with 1 hpt in wild type (Figures 6C, 6D, and 7B). The ubiquitination of UPF3 was unaffected in *mpk3*, but it was delayed to 6 hpt in *mpk6* from 2 hpt in wild type (Figures 6C, 6D, and 7B). By contrast, the induction of UPF1/UPF3 ubiquitination was unaffected by mutations in the *RESPIRATORY BURST OXIDASE HOMOLOGUE D* (*RBOHD*) and *RBOHF* genes, although UPF2 was not degraded in the flg22-treated *rbohD rbohF* mutant compared with the responses in wild type (Figures 7A and 7B; Supplemental Figure 12A). These findings indicate that the induction of UPF1/UPF3 ubiquitination requires the mitogen-activated protein kinase (MAPK) signaling cascade and the crucial early response in PTI, and that reactive oxygen species might stimulate the turnover of UPF2. Indeed, transgenic plants expressing constitutively active MPK6 (MPK6CA) showed a low level of UPF1 compared with the wild type (Supplemental Figure 12B), supporting the idea that MAPK signaling participates in the decay of UPF proteins after sensing microbial infection.

We examined the effects of SA-related defense responses on the decay event. The levels of UPF proteins were not significantly altered in the SA signaling mutants *eds1-1*, *sa induction deficient2-1* (*sid2-1*) and *nonexpresser of pr genes1* (*npr1-1*)

compared to the wild type after *Pst*DC3000 infection and flg22 treatment (Figure 7C). Exogenous treatment with BTH, a SA agonist, did not have any effect on the stability of UPF proteins in wild-type plants (Supplemental Figure 12C). The induction of UPF1/UPF3 ubiquitination upon flg22 treatment was also unaltered in these mutants (Supplemental Figure 12D). However, UPF2 persisted in *sid2-1* and *npr1-1* leaves for up to 20 h. These results suggest that the complete decay of UPF2 might involve SA-related events during a late stage of bacterial infection, which would explain the stability of UPF2 during early stages of *Pst*DC3000 infection, i.e., 0.5 to 6 hpi (Figures 2A and 7C). Based on these results, we suggest that the decay of UPF1 and UPF3 by the UPS involves as-yet unidentified events downstream of the MAPK pathway triggered by bacterial recognition rather than subsequent SA-related events.

Unannotated Fused TNL-type Transcripts Accumulate in Wild-Type Plants after Bacterial Infection

Finally, we aimed to establish a model explaining why the suppression of NMD and the resulting upregulation of

NMD-susceptible TNL transcripts lead to enhanced net immunity. The best way to illustrate this concept would be to produce a plant overexpressing the whole body of NMD-susceptible TNLs without suppressing NMD, which is impossible. As an alternative, we took previously uncharacterized fusion transcripts from RNA-seq data that were overrepresented in *upf1-5 upf3-1* and *upf3-1 upf1-5* (Supplemental Data Sets 1 and 2) and comprised four pairs of adjacent genes annotated as independent genes: *At1g57630-At1g57650*, *At2g17055-At2g17050*, *At5g38344-At5g38350*, and *At5g46490-At5g46500* (Supplemental Figures 13 and 14). The individual genes in pairs encoded N- and C-terminal fragments of TNLs, such that the fusion transcripts effectively encoded full-length TNLs (Supplemental Figure 13; Supplemental File 6). All the fusion transcripts appeared to become upregulated in wild-type plants within 30 mpi with *Pst*DC3000 except *At2g17055-At2g17050*, although the levels were not significantly different

from those under noninfection condition. Later, the fusion transcripts were over-represented within 30 hpi (Figure 8A). Except at the loci of *At5g38344* and *At5g38350*, RNAPII enrichment at the other three loci was not significantly altered by the simultaneous mutation of UPF1 and UPF3: The ChIP signals were similar in both *upf3-1 upf1-5* and wild-type plants (Figure 8B). Again, these results demonstrate that the accumulation of TNL-type transcripts is regulated by NMD and/or transcription.

Finally, to test whether these fusion transcripts were functional, we produced transgenic Arabidopsis plants expressing the *At1g57630-At1g57650* and *At5g38344-At5g38350* cDNAs under the control of the CaMV 35S promoter and terminator. Stable overexpression of these fusion transcripts, which do not retain NMD-eliciting features, conferred greater resistance to virulent *Pseudomonas* infection compared with wild-type plants (Figure 8C, left), showing that these transcripts are involved in
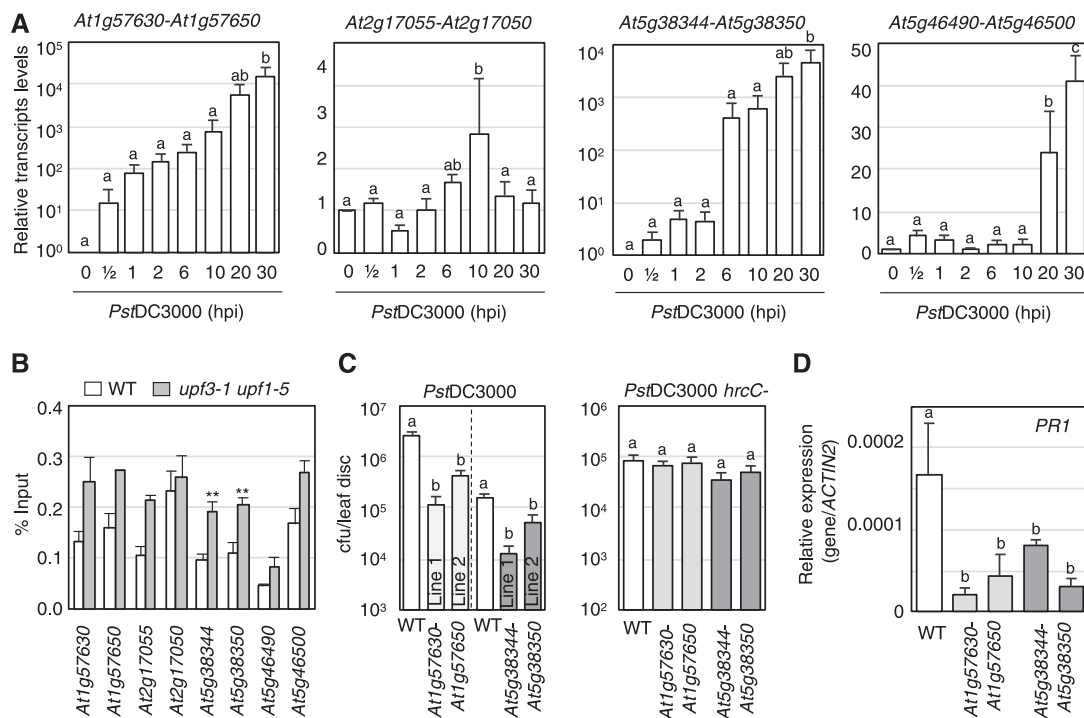

Figure 8. Stable Expression of Previously Uncharacterized Fusion Transcripts Enhances the Basal Defense Response to *P. syringae* Infection in Arabidopsis.

(A) Dynamics of fusion TNL-type *R* transcript accumulation in wild type upon *Pst*DC3000 infection. Data points are the average ± sᴅ with three biological replicates with two technical repeats (*n* = 3). Statistically significant differences are shown using different letters (i.e., a, b, c, and ab) above the bars (P < 0.01, one-way ANOVA).
(B) RNAPII enrichment at the genomic loci containing the split genes in the wild type (WT; white bars) and *upf3-1 upf1-5* (gray bars). Four independent biological experiments were performed in technical triplicates (average ± sᴇ, **P < 0.01, two-tailed Student's *t* test, *n* = 4).
(C) Bacterial growth in the wild type (WT; white bars) and in two independent transgenic Arabidopsis Col-0 plants expressing either *At1g57630-At1g57650* or *At5g38344-At5g38350* (light and dark gray bars, respectively) 3 d after *Pst*DC3000 and *Pst*DC3000 *hrcC⁻* infection. Average ± sᴇ values are plotted. Different letters (a and b) above the bars indicate statistically significant differences (P < 0.01, one-way ANOVA, *n* = 8). The numbers of *Pst*DC3000 in wild-type plants were compared with those in independent transgenic lines expressing the same fusion transcript, as different transgenic plants had been grown separately.
(D) *PR1* mRNA expression in noninfected wild-type (WT) and transgenic Arabidopsis plants used in **(C)**. Different letters (a and b) above the bars indicate statistically significant differences among the genotypes (average ± sᴅ, P < 0.05, one-way ANOVA, *n* = 3). Three biological experiments were performed with three technical repeats.

basal resistance to bacterial infection. However, the bacterial numbers of *Pst*DC3000 *hrcC*⁻ from these transgenic lines were comparable to those from wild-type plants (Figure 8C, right). In contrast to *upf3-1 upf1-5*, which produces a high level of the *PR1* transcript even before pathogen infection (Supplemental Figure 1C), the *PR1* mRNA levels were reduced in the transgenic plants in the absence of pathogen infection (Figure 8D). The conformational changes in translated NLRs crucial for NLR activation may not occur under infection by the disarmed strain and noninfection conditions (Sukarta et al., 2016). Overall, we suggest that the suppression of NMD via the degradation of UPFs and the resulting stabilization of TNL transcript levels from an early stage of bacterial infection contribute to the basal immunity of plants to virulent pathogen infection.

DISCUSSION

Microbial perception by PRRs and R proteins occurs at the forefront of the battle between plants and microbes. In this study, we demonstrated that MAMP recognition by PRRs controls the levels of *R* transcripts carrying NMD-sensitive features via the induction of UPF1/UPF3 ubiquitination, followed by their 26S-proteasome-dependent degradation at an early stage of infection.

After their export from the nucleus, virtually all mRNAs undergo mRNA surveillance processes, including NMD and miRNA-mediated gene silencing, by which only those certified as "normal" are deemed competent at translation (Eulalio et al., 2007; Lai and Eulgem, 2018). Because most FS *R* transcripts retain one of the NMD-triggering characteristics, they are thought to be either prevented from undergoing translation or immediately decayed by the NMD machinery, which may be essential for avoiding the unnecessary costs of immunity under normal growth conditions (Maekawa et al., 2011; Karasov et al., 2017). The observation that a majority of TNL and CNL genes carry NMD-sensitive features suggests that the NMD machinery and *R* genes coevolved in plants. The coexistence of both normal genes and those with NMD-regulated features in a few single *R* gene clusters (Supplemental Figure 15) suggests that gene duplication events including unequal crossing-over (Meyers et al., 2003) may have occurred before genetic drift, followed by subsequent positive selection. Such gene clusters might have evolved in land plants to facilitate the switching of *R* transcript levels (Raxwal and Riha, 2016).

Most FS *R* transcripts of the genes bearing NMD-eliciting features that we tested were highly stable in *upf3-1 upf1-5*, except for those of a few genes, supporting previous observations (Gloggnitzer et al., 2014). However, the gaps in the stability of these FS *R* transcripts between noninfected and *Pseudomonas*-infected plants were smaller than those between wild type and *upf3-1 upf1-5* under our experimental conditions. In addition, the steady-state levels of a few *R* transcripts carrying typical NMD features might also be regulated by the putative miRNA-mediated control system during *Pseudomonas* infection. Based on these findings, we speculate that NMD in *Pseudomonas*-infected plants still occurs until the UPF proteins are entirely eliminated. It is also likely that other mRNA control processes, including miRNA-mediated gene silencing, are deregulated in Arabidopsis during infection, because the intergenic pri-mRNAs may contain uORFs

or long 3′UTRs due to their weak protein-encoding capability as noncoding mRNAs or primary transcripts of small nucleolar RNAs and are thus NMD targets (Kurihara et al., 2009; Drechsel et al., 2013). The predicted NMD-sensitivity of *R* transcripts did not fully explain their actual biological NMD susceptibility, as the *R* transcripts were upregulated, unregulated, or even downregulated at a variety of time points after *Pseudomonas* infection, although most were upregulated or highly stable in the *upf3-1 upf1-5* mutant.

In addition to the FS *R* transcripts, their AS variants also predominantly accumulated in *upf* mutants (Supplemental Files 6 and 7), which suggests that the atypical cell death-like symptoms observed in *upf1-5 upf3-1* and *upf3-1 upf1-5* after virulent *Pseudomonas* infection resulted from the increased heterogenicity of the NMD-sensitive *R* transcript repertoire as well as *RPS6* (Gloggnitzer et al., 2014). Therefore, we suggest that the diversified expression of *R* genes, not their canonical functions in ETI, confers basal immunity in NMD-compromised mutants. NMD-sensitive *R* transcripts also accumulate in wild-type leaves after virulent *P. syringae* infection by suppressing NMD. How do virulent *P. syringae* strains overcome the induced barriers resulting from the accumulated R proteins? One possible explanation is that wild-type Col plants do not produce any functional R proteins capable of recognizing effectors delivered from *Pst*DC3000 and *Pca*ES4326 and are unable to trigger ETI in response to infection with these virulent pathogens, even when they accumulate high levels of NMD-sensitive *R* transcripts. If this is the case, these *R* transcripts may not function in the susceptible response in plants. During ETI, the accumulation of various sensor and helper NLRs is necessary for full immunity against avirulent pathogen infections (Jones et al., 2016; Wu et al., 2017). To achieve full immunity against a countless number of different pathogens, plants may have evolved diverse NLRs, known as the NLRome and pan-NLRome, via an arms race against a variety of pathogens (Meyers et al., 2003; van de Weyer et al., 2019). Unlike miRNAs that directly regulate the levels of their target *R* transcripts, NMD covers both AS and FS *R* transcripts as long as they carry NMD-triggering characteristics. Thus, NMD-mediated posttranscriptional regulation can diversify the expressed *R* repertoire to maximize the chances to achieve full resistance to unexpected pathogen infection. Our data do not provide details on every upregulated FS *R* transcript and its AS variants during pathogen infection, although we described their RNA-seq coverage data extracted from *upf* mutants (Supplemental Files 6 and 7). It would be interesting to monitor the dynamic changes in AS variants in real time after infection, because most splicing factor genes have AS forms, and many are also NMD-sensitive (Palusa and Reddy, 2010).

The UPS regulates diverse fundamental processes in plants, including hormonal signaling and immune responses (Kelley and Estelle, 2012; Marino et al., 2012; Dudler, 2013). The latter has been referred to as a double-edged sword, in which E3 ligases function as either positive or negative regulators of plant immunity (Marino et al., 2012). The best examples are the E3 ligases PLANT U-BOX12 (PUB12)/PUB13 and PUB22, which are involved in the decay of flagellin-induced FLS2 and EXOCYST SUBUNIT EXO70 FAMILY PROTEIN B2, respectively, resulting in attenuated plant immunity (Lu et al., 2011; Stegmann et al., 2012). The homologous

triplet PUB22/PUB23/PUB24 can dampen early immune responses stimulated by MAMPs (Trujillo et al., 2008). By contrast, the transcription of *ARABIDOPSIS TOXICOS EN LEVADURA9*, encoding a Really Interesting New Gene zinc-finger E3 ligase, is induced by a variety of external stimuli, including chitin, and the mutant shows enhanced susceptibility to *Golovinomyces cichoracearum* and reduced reactive oxygen species production after infection (Ramonell et al., 2005; Berrocal-Lobo et al., 2010). Thus, the early immune response is either suppressed or activated by ubiquitination (Marino et al., 2012). We report here that the decay of UPF1 and UPF3 via the UPS is linked to the suppression of NMD. These processes are governed by the roles of PRRs as sensors, reporting dire circumstances to the downstream components of PTI, leading to the suppression of NMD and involving the decay of even nonubiquitinated UPF2.

Unlike the well-characterized target proteins of the UPS, e.g., receptors and transcription factors, UPF proteins participate in diverse cellular processes in plants by controlling the transcriptome (Kurihara et al., 2009; Drechsel et al., 2013). Why must UPF proteins decay upon bacterial infection at the expense of such pleiotropic effects? The most likely answer is that a considerable variety of *R* proteins must accumulate during an early stage of infection to protect the host plants from attack by unpredictable pathogens before they successfully colonize the plants. When R proteins monitor their cognate avirulence proteins derived from the pathogen, plants may only have to pay a reasonable cost for subsequent immunity. If not, the accumulated R proteins can confer a defense response to plants. Thus, we suggest that the consecutive events between MAMP perception by PRRs and the accumulation of *R* transcripts are well programmed in the "black box."

The decay of UPF proteins and the accumulation of *R* transcripts occur in infected leaves at an early phase after bacterial infection. Interestingly, the significant delay in the induction of ubiquitination and subsequent decay of UPF1 in *mpk3* and *mpk6* suggests that the MAPK cascade is associated with these events. Because the *mpk3 mpk6* double mutant was lethal, we could not quantify the ubiquitination of UPF1 and UPF3 in these plants. However, the results sufficiently indicate that the MAPK cascade not only modulates transcription activators/coactivators that regulate target genes involved in plant immunity (Rasmussen et al., 2012), it also links bacterial sensing and the maintenance of *R* transcripts by participating in the induction of the ubiquitination of proteins, including UPF1 and UPF3. Therefore, our findings point to an additional layer of plasticity between the PTI and ETI by NMD.

METHODS

Plants and Pathogens

Wild-type Arabidopsis (*Arabidopsis thaliana*) Columbia-0 (Col-0) and the NMD-compromised mutants *upf1-1* (Yoine et al., 2006), *upf1-4* (Salk_022721), *upf1-5* (Salk_112922), *upf2-12* (SAIL_512_G03), *upf3-1* (Salk_025175), *upf3-2* (Salk_097931), *upf3-3* (Salk_061923), *smg7-1*, *upf1-5 upf3-1*, and *upf3-1 upf1-5* were grown in environmentally controlled growth chambers (22 ± 1°C, 16-h day [120 μmol photons m^{-2} s^{-1}]/8-h night for developmental studies or 12-h day/12-h night for

pathophysiological experiments; Hori and Watanabe, 2005; Arciga-Reyes et al., 2006; Riehs et al., 2008; Merchante et al., 2015). The *upf1-5 upf3-1* and *upf3-1 upf1-5* mutants were maintained at a high temperature (28°C, 16-h day/8-h night) until the flowering stage. The *fls2* (Salk_093905), *bak1-5*, *rbohD robhF*, *mpk3-1*, *mpk6-2*, *eds1-1*, *sid2-1*, and *npr1-1* mutants and MPK6CA transgenic plants used, as described by Parker et al. (1996), Cao et al. (1997), Nawrath and Métraux (1999), Torres et al. (2002), Wang et al. (2007); Boutrot et al. (2010), Schwessinger et al. (2011), and Hudik et al. (2014), were grown at 22°C ± 1°C with a 12-h day/12-h night photoperiod.

The ORFs of *UPF1*, *UPF2*, *UPF3*, *SMG7*, *Y14*, *MAGO*, *elF4AIII*, *BTZ1*, and *BTZ2* were cloned into CTAPi, a plant transformation vector (Rohila et al., 2004), for stable expression in Arabidopsis. The oligonucleotide sequences used to amplify the cDNA fragments are listed in Supplemental Data Set 3. Transgenic plants were produced by the floral dip method (Clough and Bent, 1998). Seeds were screened on Murashige and Skoog (MS) medium (Duchefa) containing 50 μg mL^{-1} of DL-phosphinothricin (Duchefa). T$_3$ homozygotes were isolated and used for analysis.

Freshly incubated bacterial strains *Pst*DC3000, *Pca*ES4326, *Pst*DC3000/*AvrRpm1*, *Pst*DC3000/*AvrRps4*, and *Pst*DC3000 *hrcC$^-$* in King's B medium supplemented with the appropriate antibiotics were diluted in 10 mM of MgSO$_4$ to different concentrations as follows: OD$_{600}$ = 0.05 to measure ion leakage, OD$_{600}$ = 0.01 to evaluate pathophysiological responses, and OD$_{600}$ = 0.0001 (*Pst*DC3000 and *Pca*ES4326), or OD$_{600}$ = 0.001 (*Pst*DC3000 *hrcC$^-$*) to count the number of bacteria in leaf disks. The number of bacteria in infected leaves was determined 3 d after inoculation after a typical serial dilution method, and the infected leaves were photographed on the same day.

RNA-Seq

Three-week–old Arabidopsis plants were vacuum-infiltrated for 5 min in 0.5× MS medium containing 80 μM ActD and/or 20 μM CHX and incubated in the dark for 4 h before RNA isolation (Ambion; Hori and Watanabe, 2005). After confirming the RNA purity with a bioanalyzer using the RNA 6000 Pico Kit (Agilent), the total RNA was processed for mRNA sequencing library preparation using a TruSeq Stranded mRNA Sample Preparation Kit according to the manufacturer's instructions (Illumina). In brief, mRNAs were isolated from 400 ng of total RNA with RNA purification beads using poly(A) capture followed by enzyme shearing. After first- and second-strand cDNA synthesis, A-tailing and end repair were performed for the ligation of proprietary primers incorporating unique sequencing adaptors with an index for tracking Illumina reads from multiplexed samples run on a single sequencing lane. All samples were processed in two biological replicates per genotype, each from individual plants. For each library, an insert size of ~270 bp was confirmed with a bioanalyzer, and the library was quantified by RT-PCR using the CFX96 System (BioRad). Each library was sequenced for 75-bp paired-end reads with a NextSeq500 High Output 150 Cycle Kit on the NextSeq500 platform (Illumina).

The raw image data were transformed by base-calling into sequence data and stored in FASTQ format. The RNA-seq data were aligned by the softwares TopHat2 and BowTie2 to detect the canonical and noncanonical intron motifs (Langmead and Salzberg, 2012; Kim et al., 2013). Unaligned reads using the above platforms were mapped by the software BLAST (Trapnell et al., 2010). AS events were extracted from The Arabidopsis Information Resource 10 (TAIR10) gene models (www.arabidopsis.org). To evaluate NMD-triggering features (see "Evaluation of *R* Transcripts for NMD-Sensitive Features"), the data sets were mapped in the Integrative Genomics Viewer browser (Robinson et al., 2011; Thorvaldsdóttir et al., 2013). To quantify the total transcript mass in fragments per kilobase of transcript per million mapped reads, biological replicates of ActD-treated wild-type Col-0, ActD/CHX-treated wild-type Col-0, *upf1-5*, *upf3-1*, and *upf3-1 upf1-5* were separately aligned with the Arabidopsis TAIR10 gene model using the Cufflinks package (Saeed et al., 2003).

Evaluation of *R* Transcripts for NMD-Sensitive Features

Although many normal-looking mRNAs can be regulated by NMD via low translation efficiency of the main ORF or out-of-frame translation due to ribosome read-through (Celik et al., 2017), we ruled out these possibilities due to the absence of sufficient evidence in Arabidopsis genes. We examined three NMD-triggering features to judge whether the individual TNL or CNL transcripts are putatively NMD-regulated:

Intron in the 3′UTR

Introns occurring more than 55 nucleotides downstream of the termination-codon trigger NMD, by which the ribosome-bound UPF1 and EJC-bound UPF2–UPF3 complex are well spaced to activate UPF1 (Kertész et al., 2006; Nyikó et al., 2013; Le Hir et al., 2016).

Long 3′UTR

Long 3′UTR (≥350 nucleotides)-containing transcripts are also NMD targets in Arabidopsis (Kertész et al., 2006; Kerényi et al., 2008; Kalyna et al., 2012), wherein UPF1, which otherwise falls off the normal mRNA template due to its own ATPase activity, binds in a size-dependent manner for the phosphorylation and activation of NMD (Kurosaki et al., 2014; Peccarelli and Kebaara, 2014).

uORFs

Although uORF-driven NMD has also been considered an EJC type, exactly how it can trigger NMD is still unclear, because the translation of uORFs is often leaky. Approximately 20% of Arabidopsis genes contain uORFs (Kochetov et al., 2002) of which only up to 2% are putative NMD targets that contain uORFs encoding ≥ 35-amino acid peptides for stable expression. (Nyikó et al., 2009, 2013). The *MAGNESIUM/PROTON EXCHANGER* (*AtMHX*) uORF, encoding a 13-amino–acid peptide, induces NMD in a downstream intron-dependent manner (Saul et al., 2009). Here, however, we considered CNL and TNL transcripts containing only uORFs encoding peptide(s) ≥ 35 amino acids as NMD targets based on general observations (Nyikó et al., 2009). The transcripts carrying uORFs that overlap with the authentic initiation codons were also considered to have putative NMD-sensitive features because this event showed strong correlations with sensitivity to NMD, even in the transcripts with uORFs encoding ≤ 35 amino acids (Kalyna et al., 2012).

RNA Analysis

Leaves of 4-week–old Arabidopsis (~0.1 g) infiltrated with the *Pst*DC3000 strain or 80 μM of ActD/20 μM CHX were harvested at the indicated time points after treatment. RNA extracted from the leaves following the manufacturer's instructions (TRIzol reagent; Thermo Fisher Scientific). TURBO DNase (2 units; Thermo Fisher Scientific) was used to remove contaminating genomic DNA. After phenol/chloroform/isoamyl alcohol extraction, the purified RNA was dissolved in diethyl pyrocarbonate-treated water. Five micrograms of total RNA were used to synthesize first-strand cDNA by SuperScript-II RTase (Thermo Fisher Scientific), and the first-strand cDNA was diluted 10-fold for standard RT-PCR or RT-qPCR. RT-qPCR was performed with SYBR Premix Ex Taq (TaKaRa Bio) as described previously by Jung et al. (2009). All experiments were performed in three biological replicates with two or three technical repeats. The oligonucleotide sequences used in this study are presented in Supplemental Data Set 3.

Quantification of Cell-Death–Like Responses

Electrolyte leakage measurements were performed to quantify the hypersensitive response in plants after infection (Sohn et al., 2012). After infiltrating *Pst*DC3000 into the leaves of wild-type and mutant plants, 10 leaf disks per biological replicate ($n = 4$) were collected from the infected leaves of different plants, rinsed with distilled water for 30 min, and submerged in 2 mM of $MgSO_4$. Conductivity was measured from 1 to 36 hpi with a LAQUAtwin Compact Water Quality Meter (HORIBA Life Science Solutions).

flg22 Treatment and SA Measurement

flg22 (1 μM; Peptron) was infiltrated into Arabidopsis leaves, and the treated plants were transferred to a growth chamber (22 ± 1°C, 12-h day/12-h night). The leaves were collected at the indicated time points after treatment to examine the levels of UPF proteins. Free-SA levels were also quantified using HPLC coupled with a fluorescence detector (Agilent) as described previously by Seskar et al. (1998) and Jung et al. (2009).

Monoclonal and Polyclonal Antibodies against UPF Proteins, IP, and Immunoblot Analysis

After analysis of the UPF1, UPF2, and UPF3 primary sequences using the software package SEAL (http://www.ab-mart.com), four peptide fragments per protein were designed to yield monoclonal antibodies (Supplemental Figure 16). After vigorous tests for 3 to 4 antibodies raised from each peptide using enzyme-linked immunosorbent assay and immunoblot analysis, one epitope each from the four peptides against each protein appeared to generate a specific antibody: 41-GSPTAWPTPSDS-52 (UPF1), UPF2 (933-ENGEAHGEESDS-944) and UPF3 (192-NKPSPRPSKRNS-203). These antibodies were used for further immunoblot and IP analyses. The specificity and sensitivity of the selected monoclonal antibodies were verified by immunoblotting using different *upf1*, *upf2*, and *upf3* mutant alleles (Supplemental Figure 6).

GST-UPF1(1-232), covering the N-terminal and Cys- and His-rich domains, was bacterially expressed and purified by glutathione-agarose chromatography (Green and Sambrook, 2012), followed by extraction from SDS-polyacrylamide gels, and used to raise an anti-UPF1 rabbit polyclonal antibody (Youngin Biotech).

For IP, leaf samples were ground in extraction buffer containing 20 mM of Tris-Cl at pH 8.0, 1 mM of EDTA, 100 mM of NaCl (Figure 5; Supplemental Figure 9) or 150 mM of NaCl (Figures 3, 6, and 7; Supplemental Figures 8 and 12), 1 mM of PMSF, and 1× proteinase inhibitor, and clarified at 15,000*g* for 10 min at 4°C. The homogenate was incubated with protein G-magnetic beads (Invitrogen) that were coated with the α-UPF1, α-UPF2, or α-UPF3 monoclonal antibody for 1 h at 4°C. The immune complex on the magnetic beads was washed five times in buffer containing 20 mM of Tris-Cl at pH 8.0, 1 mM of EDTA, 100 mM (or 150 mM for high stringency) of NaCl, and 0.5% (v/v) Triton X-100, resuspended in SDS sample buffer, and loaded on SDS-polyacrylamide gels for subsequent immunoblot analysis.

Finely ground leaf powder was homogenized in an equal volume of protein extraction buffer containing 20 mM of Tris-HCl at pH 7.5, 1 mM of EDTA, 150 mM of NaCl, 0.1% (v/v) Triton X-100, 0.1% (w/v) SDS, 5 mM of dithiothreitol, and 1× proteinase inhibitor (Roche Applied Science) and loaded onto SDS-polyacrylamide gels after clarification for immunoblot analysis as described by Green and Sambrook (2012). The antibodies and manufacturers were as follows: α-UBQ (AS08 307, Agrisera), α-PR1 (AS10 687, Agrisera), and α-PAP (P1291; Sigma-Aldrich). The dilution of primary antibodies used in this study was 1:5,000. The signal was visualized with a chemiluminescent substrate (Intron).

ChIP-qPCR

Nuclei from the leaves of 4-week–old wild-type and *upf3-1 upf1-5* plants were extracted and purified as described in Jaskiewicz et al. (2011). The purified nuclei were resuspended in nucleus lysis buffer (50 mM of Tris-Cl at

pH 8.0, 10 mM of EDTA, 1% [w/v] SDS, and 1× proteinase inhibitor [Roche Applied Science]), and the resulting chromatin was sheared by sonication to obtain fragment sizes ranging from 200 to 800 bp (Biorupter; Diagenode). The ChIP assay was performed using an anti-C-terminal domain (phospho-S5) antibody (ab5131; Abcam) as described by the manufacturer (Pierce Agarose ChIP Kit; Thermo Fisher Scientific). RNAPII enrichment between the transcription start sites and translation initiation sites of representative TNL- and CNL-type *R* genes was determined by RT-qPCR and calculated by the percent input method (Lin et al., 2012). The primers used in this study are listed in Supplemental Data Set 3.

Statistical Analysis

One-way ANOVA with a post hoc Tukey honest significant difference test was used for multiple comparisons. To analyze significant differences between the control and treatment groups, a two-tailed Student's *t* test was employed in this study. The sample size (*n*) and type of error bar are indicated in the figure legends. All pathophysiological experiments were performed in at least triplicate. The results of all statistical analyses performed in this study are presented in Supplemental Data Sets 4 and 5.

Accession Numbers

The accession numbers for the genes examined and discussed in this article are as follows: *ACTIN2* (*At3g18780*), *BTZ1* (*At1g80000*), *BTZ2* (*At1g15280*), *EDS1* (*At3g48090*), *eIF4AIII* (*At3g19760*), *FLG22-INDUCED RECEPTOR-LIKE KINASE1* (*At2g19190*), *ICS1*/SID2 (*At1g74710*), *LPEAT2* (*At2g45670*), *MAGO* (*At1g02140*), *MPK3* (*At3g45640*), *MPK6* (*At2g43790*), *FLG22-INDUCED RECEPTOR-LIKE KINASE1, NDR1-HIN1-LIKE10* (*At2g35980*), *NPR1* (*At1g64280*), *PAD4* (*At3g52430*), *PR1* (*At2g14610*), *RBOHD* (*At5g47910*), *RBOHF* (*At1g64060*), *RPM1* (*At3g07040*), *RPP5* (*At4g16950*), *RPP7* (*At1g58602*), *RPS2* (*At4g26090*), *RPS4* (*At5g45250*), *RPS5* (*At1g12220*), *RPS6* (*At5g46740*), *RRS1* (*At5g45260*), *RSG2* (*At5g43730*), *SIKIC3* (*At4g16960*), *SMG7* (*At5g19400*), *SNC1* (*At4g16890*), *SOC3* (*At1g17600*), *SUMM2* (*At1g12280*), *UPF1* (*At5g47010*), *UPF2* (*At2g39260*), *UPF3* (*At1g33980*), and *Y14* (*At1g51510*).

RNA-seq data have been deposited in The National Agricultural Biotechnology Information Center (http://nabic.rda.go.kr/) under accession numbers NN-5098, NN-5102, NN-5103, NN-5104, and NN-5105.

Supplemental Data

Supplemental Figure 1. *upf1-5 upf3-1* and *upf3-1 upf1-5* exhibit severe necrotic responses and enhanced immune responses against infection with virulent *Pseudomonas* strains.

Supplemental Figure 2. Representative *R* transcripts that accumulated in the leaves of NMD-compromised mutants.

Supplemental Figure 3. Stability of the mRNAs of TNLs and CNLs in wild-type and *upf3-1 upf1-5* plants.

Supplemental Figure 4. RNAPII enrichment at FS *R* genes in wild-type and *upf3-1 upf1-5* plants.

Supplemental Figure 5. Upregulation of the FS natural *UPF1*, *UPF3*, and *SMG7* transcripts and AS versions of *UPF1* and *UPF2* in wild-type leaves during infection.

Supplemental Figure 6. Morphology of the wild-type and NMD-compromised mutants and the specificities of monoclonal antibodies used in this study.

Supplemental Figure 7. Stability of UPF1 in wild-type leaves infected with different *P. syringae* strains.

Supplemental Figure 8. Levels of UPF proteins in the immune complexes shown in Figures 3B, 3C, and 6C.

Supplemental Figure 9. UPF2 physically associates with UPF3 regardless of bacterial infection.

Supplemental Figure 10. Steady-state levels and stability of the mRNAs of TNLs and CNLs in wild-type leaves infected with a virulent *Pst*DC3000 strain.

Supplemental Figure 11. Steady-state levels and stability of putative miRNA-target *R* transcripts.

Supplemental Figure 12. Induction of UPF1 and UPF3 ubiquitination occurs independently of reactive oxygen species burst or SA signaling.

Supplemental Figure 13. Structures of the fusion transcripts encoded by two separately annotated genes and their protein products.

Supplemental Figure 14. RNA-seq coverage plots of the *At1g57630-57650* fusion transcript.

Supplemental Figure 15. Physical locations of Arabidopsis *R* genes.

Supplemental Figure 16. Amino acid sequences of UPF1, UPF2, and UPF3.

Supplemental Data Set 1. Read counts and fragments per kilobase of transcript per million mapped reads values of the Arabidopsis NLR genes determined by RNA-seq in the wild-type and NMD-compromised mutants 4 h after ActD treatment.

Supplemental Data Set 2. NMD-sensitive features in the TNL- and CNL-type genes expressed in Arabidopsis leaves

Supplemental Data Set 3. Oligonucleotides used in this study.

Supplemental Data Set 4. Statistical analysis of the results of shown in Figures 1, 2, 4, and 8.

Supplemental Data Set 5. Statistical analysis of the results of shown in the Supplemental Figures 1, 2, 4, 10, and 11.

Supplemental File 1. Nucleotide sequences of the genomic DNA region of each TNL-type gene in the Arabidopsis genome.

Supplemental File 2. Genomic DNA sequences of Arabidopsis CNL-type genes.

Supplemental File 3. Nucleotide sequences of the FS natural transcripts and the AS variants of each TNL-type gene obtained by RNA-seq analysis.

Supplemental File 4. Transcripts of the CNL-type genes identified by RNA-seq analysis.

Supplemental File 5. Legends of Supplemental Files 1 and 2.

Supplemental File 6. The 85 FS natural transcripts and their AS variants from the Arabidopsis TNL genes expressed in leaves of the wild-type and *upf* mutants.

Supplemental File 7. The 43 FS natural transcripts and their AS variants from the Arabidopsis CNL genes expressed in leaves of the wild-type and *upf* mutants.

AUTHOR CONTRIBUTIONS

H.W.J. and S.H.K. conceived the study, designed the experiments, analyzed and interpreted the data, and wrote the article; H.W.J., G.K.P., G.Y.J., Y.J.L., K.H.S., A.S., E.S.C., E.L., K.M.K., S.H.Y., J.S.J., and S.C.L. performed the experiments.

REFERENCES

Alcázar, R., and Parker, J.E. (2011). The impact of temperature on balancing immune responsiveness and growth in Arabidopsis. Trends Plant Sci. **16:** 666–675.

Arciga-Reyes, L., Wootton, L., Kieffer, M., and Davies, B. (2006). UPF1 is required for nonsense-mediated mRNA decay (NMD) and RNAi in Arabidopsis. Plant J. **47:** 480–489.

Banihashemi, L., Wilson, G.M., Das, N., and Brewer, G. (2006). Upf1/Upf2 regulation of 3′ untranslated region splice variants of AUF1 links nonsense-mediated and A+U–rich element-mediated mRNA decay. Mol. Cell. Biol. **26:** 8743–8754.

Berrocal-Lobo, M., Stone, S., Yang, X., Antico, J., Callis, J., Ramonell, K.M., and Somerville, S. (2010). ATL9, a RING zinc finger protein with E3 ubiquitin ligase activity implicated in chitin- and NADPH oxidase-mediated defense responses. PLoS One **5:** e14426.

Boccara, M., Sarazin, A., Thiébeauld, O., Jay, F., Voinnet, O., Navarro, L., and Colot, V. (2015). Correction: The Arabidopsis miR472-RDR6 silencing pathway modulates PAMP- and effector-triggered immunity through the post-transcriptional control of disease resistance genes. PLoS Pathog. **11:** e1004814.

Boutrot, F., Segonzac, C., Chang, K.N., Qiao, H., Ecker, J.R., Zipfel, C., and Rathjen, J.P. (2010). Direct transcriptional control of the Arabidopsis immune receptor FLS2 by the ethylene-dependent transcription factors EIN3 and EIL1. Proc. Natl. Acad. Sci. USA **107:** 14502–14507.

Braten, O., et al. (2016). Numerous proteins with unique characteristics are degraded by the 26S proteasome following mono-ubiquitination. Proc. Natl. Acad. Sci. USA **113:** E4639–E4647.

Bull, C.T., Manceau, C., Lydon, J., Kong, H., Vinatzer, B.A., and Fischer-Le Saux, M. (2010). *Pseudomonas cannabina* pv. *cannabina* pv. nov., and *Pseudomonas cannabina* pv. *alisalensis* (Cintas Koike and Bull, 2000) comb. nov., are members of the emended species *Pseudomonas cannabina* (ex Sutic & Dowson 1959) Gardan, Shafik, Belouin, Brosch, Grimont & Grimont 1999. Syst. Appl. Microbiol. **33:** 105–115.

Cai, Q., Liang, C., Wang, S., Hou, Y., Gao, L., Liu, L., He, W., Ma, W., Mo, B., and Chen, X. (2018). The disease resistance protein SNC1 represses the biogenesis of microRNAs and phased siRNAs. Nat. Commun. **9:** 5080.

Cao, H., Glazebrook, J., Clarke, J.D., Volko, S., and Dong, X. (1997). The Arabidopsis NPR1 gene that controls systemic acquired resistance encodes a novel protein containing ankyrin repeats. Cell **88:** 57–63.

Carstens, M., McCrindle, T.K., Adams, N., Diener, A., Guzha, D.T., Murray, S.L., Parker, J.E., Denby, K.J., and Ingle, R.A. (2014). Increased resistance to biotrophic pathogens in the Arabidopsis constitutive induced resistance1 mutant is EDS1 and PAD4-dependent and modulated by environmental temperature. PLoS One **9:** e109853.

Celik, A., Baker, R., He, F., and Jacobson, A. (2017). High-resolution profiling of NMD targets in yeast reveals translational fidelity as a basis for substrate selection. RNA **23:** 735–748.

Chisholm, S.T., Coaker, G., Day, B., and Staskawicz, B.J. (2006). Host-microbe interactions: Shaping the evolution of the plant immune response. Cell **124:** 803–814.

Ciechanover, A., and Stanhill, A. (2014). The complexity of recognition of ubiquitinated substrates by the 26S proteasome. Biochim. Biophys. Acta **1843:** 86–96.

Clough, S.J., and Bent, A.F. (1998). Floral dip: A simplified method for Agrobacterium-mediated transformation of *Arabidopsis thaliana*. Plant J. **16:** 735–743.

Degtiar, E., Fridman, A., Gottlieb, D., Vexler, K., Berezin, I., Farhi, R., Golani, L., and Shaul, O. (2015). The feedback control of UPF3 is crucial for RNA surveillance in plants. Nucleic Acids Res. **43:** 4219–4235.

DeYoung, B.J., and Innes, R.W. (2006). Plant NBS-LRR proteins in pathogen sensing and host defense. Nat. Immunol. **7:** 1243–1249.

Dinesh-Kumar, S.P., and Baker, B.J. (2000). Alternatively spliced N resistance gene transcripts: Their possible role in tobacco mosaic virus resistance. Proc. Natl. Acad. Sci. USA **97:** 1908–1913.

Drechsel, G., Kahles, A., Kesarwani, A.K., Stauffer, E., Behr, J., Drewe, P., Rätsch, G., and Wachter, A. (2013). Nonsense-mediated decay of alternative precursor mRNA splicing variants is a major determinant of the Arabidopsis steady state transcriptome. Plant Cell **25:** 3726–3742.

Dudler, R. (2013). Manipulation of host proteasomes as a virulence mechanism of plant pathogens. Annu. Rev. Phytopathol. **51:** 521–542.

Eulalio, A., Behm-Ansmant, I., and Izaurralde, E. (2007). P bodies: At the crossroads of post-transcriptional pathways. Nat. Rev. Mol. Cell Biol. **8:** 9–22.

Filichkin, S.A., Cumbie, J.S., Dharmawardhana, P., Jaiswal, P., Chang, J.H., Palusa, S.G., Reddy, A.S., Megraw, M., and Mockler, T.C. (2015). Environmental stresses modulate abundance and timing of alternatively spliced circadian transcripts in Arabidopsis. Mol. Plant **8:** 207–227.

Garcia, D., Garcia, S., and Voinnet, O. (2014). Nonsense-mediated decay serves as a general viral restriction mechanism in plants. Cell Host Microbe **16:** 391–402.

Gloggnitzer, J., Akimcheva, S., Srinivasan, A., Kusenda, B., Riehs, N., Stampfl, H., Bautor, J., Dekrout, B., Jonak, C., Jiménez-Gómez, J.M., Parker, J.E., and Riha, K. (2014). Nonsense-mediated mRNA decay modulates immune receptor levels to regulate plant antibacterial defense. Cell Host Microbe **16:** 376–390.

Green, M.R., and Sambrook, J. (2012). Molecular Cloning: A Laboratory Manual, Fourth Edition. (Cold Spring Harbor, NY: Cold Spring Harbor Laboratory Press).

Halter, T., and Navarro, L. (2015). Multilayer and interconnected post-transcriptional and co-transcriptional control of plant NLRs. Curr. Opin. Plant Biol. **26:** 127–134.

Heidrich, K., Tsuda, K., Blanvillain-Baufumé, S., Wirthmueller, L., Bautor, J., and Parker, J.E. (2013). Arabidopsis TNL-WRKY domain receptor RRS1 contributes to temperature-conditioned RPS4 auto-immunity. Front Plant Sci **4:** 403.

Hori, K., and Watanabe, Y. (2005). UPF3 suppresses aberrant spliced mRNA in Arabidopsis. Plant J. **43:** 530–540.

Hudik, E., Berriri, S., Hirt, H., and Colcombet, J. (2014). Identification of constitutively active AtMPK6 mutants using a functional screen in *Saccharomyces cerevisiae*. Methods Mol. Biol. **1171:** 67–77.

Jaskiewicz, M., Peterhansel, C., and Conrath, U. (2011). Detection of histone modifications in plant leaves. J. Vis. Exp. **55:** 3096.

Jeong, H.J., Kim, Y.J., Kim, S.H., Kim, Y.H., Lee, I.J., Kim, Y.K., and Shin, J.S. (2011). Nonsense-mediated mRNA decay factors, UPF1 and UPF3, contribute to plant defense. Plant Cell Physiol. **52:** 2147–2156.

Jones, J.D., and Dangl, J.L. (2006). The plant immune system. Nature **444:** 323–329.

Jones, J.D., Vance, R.E., and Dangl, J.L. (2016). Intracellular innate immune surveillance devices in plants and animals. Science **354:** aaf6395.

Jung, H.W., Tschaplinski, T.J., Wang, L., Glazebrook, J., and Greenberg, J.T. (2009). Priming in systemic plant immunity. Science **324:** 89–91.

Kalyna, M., et al. (2012). Alternative splicing and nonsense-mediated decay modulate expression of important regulatory genes in Arabidopsis. Nucleic Acids Res. **40:** 2454–2469.

Karasov, T.L., Chae, E., Herman, J.J., and Bergelson, J. (2017). Mechanisms to mitigate the trade-off between growth and defense. Plant Cell **29:** 666–680.

Kelley, D.R., and Estelle, M. (2012). Ubiquitin-mediated control of plant hormone signaling. Plant Physiol. **160:** 47–55.

Kerényi, Z., Mérai, Z., Hiripi, L., Benkovics, A., Gyula, P., Lacomme, C., Barta, E., Nagy, F., and Silhavy, D. (2008). Inter-kingdom conservation of mechanism of nonsense-mediated mRNA decay. EMBO J. **27:** 1585–1595.

Kertész, S., Kerényi, Z., Mérai, Z., Bartos, I., Pálfy, T., Barta, E., and Silhavy, D. (2006). Both introns and long 3′-UTRs operate as cis-acting elements to trigger nonsense-mediated decay in plants. Nucleic Acids Res. **34:** 6147–6157.

Kesarwani, A.K., Lee, H.C., Ricca, P.G., Sullivan, G., Faiss, N., Wagner, G., Wunderling, A., and Wachter, A. (2019). Multifactorial and species-specific feedback regulation of the RNA surveillance pathway nonsense-mediated decay in plants. Plant Cell Physiol. **60:** 1986–1999.

Kim, D., Pertea, G., Trapnell, C., Pimentel, H., Kelley, R., and Salzberg, S.L. (2013). TopHat2: accurate alignment of transcriptomes in the presence of insertions, deletions and gene fusions. Genome Biol. **14:** R36.

Kim, S.H., Koroleva, O.A., Lewandowska, D., Pendle, A.F., Clark, G.P., Simpson, C.G., Shaw, P.J., and Brown, J.W. (2009). Aberrant mRNA transcripts and the nonsense-mediated decay proteins UPF2 and UPF3 are enriched in the Arabidopsis nucleolus. Plant Cell **21:** 2045–2057.

Kim, V.N., Kataoka, N., and Dreyfuss, G. (2001). Role of the nonsense-mediated decay factor hUpf3 in the splicing-dependent exon-exon junction complex. Science **293:** 1832–1836.

Kochetov, A.V., Syrnik, O.A., Rogozin, I.B., Glazko, G.V., Komarova, M.L., and Shumnyĭ, V.K. (2002). Context organization of mRNA 5′-untranslated regions of higher plants [in Russian]. Mol. Biol. (Mosk.) **36:** 649–656.

Kurihara, Y., et al. (2009). Genome-wide suppression of aberrant mRNA-like noncoding RNAs by NMD in Arabidopsis. Proc. Natl. Acad. Sci. USA **106:** 2453–2458.

Kurosaki, T., Li, W., Hoque, M., Popp, M.W., Ermolenko, D.N., Tian, B., and Maquat, L.E. (2014). A post-translational regulatory switch on UPF1 controls targeted mRNA degradation. Genes Dev. **28:** 1900–1916.

Lai, Y., and Eulgem, T. (2018). Transcript-level expression control of plant NLR genes. Mol. Plant Pathol. **19:** 1267–1281.

Langmead, B., and Salzberg, S.L. (2012). Fast gapped-read alignment with BowTie 2. Nat. Methods **9:** 357–359.

Le Hir, H., Saulière, J., and Wang, Z. (2016). The exon junction complex as a node of post-transcriptional networks. Nat. Rev. Mol. Cell Biol. **17:** 41–54.

Li, X., Clarke, J.D., Zhang, Y., and Dong, X. (2001). Activation of an EDS1-mediated R-gene pathway in the snc1 mutant leads to constitutive, NPR1-independent pathogen resistance. Mol. Plant Microbe Interact. **14:** 1131–1139.

Li, X., Kapos, P., and Zhang, Y. (2015). NLRs in plants. Curr. Opin. Immunol. **32:** 114–121.

Lin, X., Tirichine, L., and Bowler, C. (2012). Protocol: Chromatin immunoprecipitation (ChIP) methodology to investigate histone modifications in two model diatom species. Plant Methods **8:** 48.

Lu, D., Lin, W., Gao, X., Wu, S., Cheng, C., Avila, J., Heese, A., Devarenne, T.P., He, P., and Shan, L. (2011). Direct ubiquitination of pattern recognition receptor FLS2 attenuates plant innate immunity. Science **332:** 1439–1442.

Maekawa, T., Kufer, T.A., and Schulze-Lefert, P. (2011). NLR functions in plant and animal immune systems: so far and yet so close. Nat. Immunol. **12:** 817–826.

Marino, D., Peeters, N., and Rivas, S. (2012). Ubiquitination during plant immune signaling. Plant Physiol. **160:** 15–27.

Mérai, Z., Benkovics, A.H., Nyikó, T., Debreczeny, M., Hiripi, L., Kerényi, Z., Kondorosi, É., and Silhavy, D. (2013). The late steps of plant nonsense-mediated mRNA decay. Plant J. **73:** 50–62.

Merchante, C., Brumos, J., Yun, J., Hu, Q., Spencer, K.R., Enríquez, P., Binder, B.M., Heber, S., Stepanova, A.N., and Alonso, J.M. (2015). Gene-specific translation regulation mediated by the hormone-signaling molecule EIN2. Cell **163:** 684–697.

Meyers, B.C., Kozik, A., Griego, A., Kuang, H., and Michelmore, R.W. (2003). Genome-wide analysis of NBS-LRR-encoding genes in Arabidopsis. Plant Cell **15:** 809–834.

Nawrath, C., and Métraux, J.P. (1999). Salicylic acid induction-deficient mutants of Arabidopsis express PR-2 and PR-5 and accumulate high levels of camalexin after pathogen inoculation. Plant Cell **11:** 1393–1404.

Nicaise, V., Roux, M., and Zipfel, C. (2009). Recent advances in PAMP-triggered immunity against bacteria: pattern recognition receptors watch over and raise the alarm. Plant Physiol. **150:** 1638–1647.

Nyikó, T., Kerényi, F., Szabadkai, L., Benkovics, A.H., Major, P., Sonkoly, B., Mérai, Z., Barta, E., Niemiec, E., Kufel, J., and Silhavy, D. (2013). Plant nonsense-mediated mRNA decay is controlled by different autoregulatory circuits and can be induced by an EJC-like complex. Nucleic Acids Res. **41:** 6715–6728.

Nyikó, T., Sonkoly, B., Mérai, Z., Benkovics, A.H., and Silhavy, D. (2009). Plant upstream ORFs can trigger nonsense-mediated mRNA decay in a size-dependent manner. Plant Mol. Biol. **71:** 367–378.

Palma, K., Thorgrimsen, S., Malinovsky, F.G., Fiil, B.K., Nielsen, H.B., Brodersen, P., Hofius, D., Petersen, M., and Mundy, J. (2010). Autoimmunity in Arabidopsis acd11 is mediated by epigenetic regulation of an immune receptor. PLoS Pathog. **6:** e1001137.

Palusa, S.G., and Reddy, A.S. (2010). Extensive coupling of alternative splicing of pre-mRNAs of serine/arginine (SR) genes with nonsense-mediated decay. New Phytol. **185:** 83–89.

Parker, J.E., Holub, E.B., Frost, L.N., Falk, A., Gunn, N.D., and Daniels, M.J. (1996). Characterization of eds1, a mutation in Arabidopsis suppressing resistance to *Peronospora parasitica* specified by several different RPP genes. Plant Cell **8:** 2033–2046.

Peccarelli, M., and Kebaara, B.W. (2014). Regulation of natural mRNAs by the nonsense-mediated mRNA decay pathway. Eukaryot. Cell **13:** 1126–1135.

Ramonell, K., Berrocal-Lobo, M., Koh, S., Wan, J., Edwards, H., Stacey, G., and Somerville, S. (2005). Loss-of-function mutations in chitin responsive genes show increased susceptibility to the powdery mildew pathogen *Erysiphe cichoracearum*. Plant Physiol. **138:** 1027–1036.

Rasmussen, M.W., Roux, M., Petersen, M., and Mundy, J. (2012). MAP kinase cascades in Arabidopsis innate immunity. Front Plant Sci **3:** 169.

Raxwal, V.K., and Riha, K. (2016). Nonsense mediated RNA decay and evolutionary capacitance. Biochim. Biophys. Acta **1859:** 1538–1543.

Rayson, S., Arciga-Reyes, L., Wootton, L., De Torres Zabala, M., Truman, W., Graham, N., Grant, M., and Davies, B. (2012). A role for nonsense-mediated mRNA decay in plants: Pathogen responses are induced in *Arabidopsis thaliana* NMD mutants. PLoS One **7:** e31917.

Rebbapragada, I., and Lykke-Andersen, J. (2009). Execution of nonsense-mediated mRNA decay: What defines a substrate? Curr. Opin. Cell Biol. **21:** 394–402.

Riehs, N., Akimcheva, S., Puizina, J., Bulankova, P., Idol, R.A., Siroky, J., Schleiffer, A., Schweizer, D., Shippen, D.E., and Riha, K. (2008). Arabidopsis SMG7 protein is required for exit from meiosis. J. Cell Sci. **121:** 2208–2216.

Riehs-Kearnan, N., Gloggnitzer, J., Dekrout, B., Jonak, C., and Riha, K. (2012). Aberrant growth and lethality of Arabidopsis deficient in nonsense-mediated RNA decay factors is caused by autoimmune-like response. Nucleic Acids Res. **40:** 5615–5624.

Robinson, J.T., Thorvaldsdóttir, H., Winckler, W., Guttman, M., Lander, E.S., Getz, G., and Mesirov, J.P. (2011). Integrative genomics viewer. Nat. Biotechnol. **29:** 24–26.

Rohila, J.S., Chen, M., Cerny, R., and Fromm, M.E. (2004). Improved tandem affinity purification tag and methods for isolation of protein heterocomplexes from plants. Plant J. **38:** 172–181.

Saeed, A.I., et al. (2003). TM4: A free, open-source system for microarray data management and analysis. Biotechniques **34:** 374–378.

Saul, H., et al. (2009). The upstream open reading frame of the Arabidopsis AtMHX gene has a strong impact on transcript accumulation through the nonsense-mediated mRNA decay pathway. Plant J. **60:** 1031–1042.

Schweingruber, C., Rufener, S.C., Zünd, D., Yamashita, A., and Mühlemann, O. (2013). Nonsense-mediated mRNA decay—mechanisms of substrate mRNA recognition and degradation in mammalian cells. Biochim. Biophys. Acta **1829:** 612–623.

Schwessinger, B., Roux, M., Kadota, Y., Ntoukakis, V., Sklenar, J., Jones, A., and Zipfel, C. (2011). Phosphorylation-dependent differential regulation of plant growth, cell death, and innate immunity by the regulatory receptor-like kinase BAK1. PLoS Genet. **7:** e1002046.

Seskar, M., Shulaev, V., and Raskin, I. (1998). Endogenous methyl salicylate in pathogen-inoculated tobacco plants. Plant Physiol. **116:** 387–392.

Shabek, N., Herman-Bachinsky, Y., Buchsbaum, S., Lewinson, O., Haj-Yahya, M., Hejjaoui, M., Lashuel, H.A., Sommer, T., Brik, A., and Ciechanover, A. (2012). The size of the proteasomal substrate determines whether its degradation will be mediated by mono- or polyubiquitylation. Mol. Cell **48:** 87–97.

Shaul, O. (2015). Unique aspects of plant nonsense-mediated mRNA decay. Trends Plant Sci. **20:** 767–779.

Shi, C., Baldwin, I.T., and Wu, J. (2012). Arabidopsis plants having defects in nonsense-mediated mRNA decay factors UPF1, UPF2, and UPF3 show photoperiod-dependent phenotypes in development and stress responses. J. Integr. Plant Biol. **54:** 99–114.

Shirano, Y., Kachroo, P., Shah, J., and Klessig, D.F. (2002). A gain-of-function mutation in an Arabidopsis Toll Interleukin1 receptor-nucleotide binding site-leucine-rich repeat type R gene triggers defense responses and results in enhanced disease resistance. Plant Cell **14:** 3149–3162.

Shivaprasad, P.V., Chen, H.M., Patel, K., Bond, D.M., Santos, B.A., and Baulcombe, D.C. (2012). A microRNA superfamily regulates nucleotide binding site-leucine-rich repeats and other mRNAs. Plant Cell **24:** 859–874.

Sobell, H.M. (1985). Actinomycin and DNA transcription. Proc. Natl. Acad. Sci. USA **82:** 5328–5331.

Sohn, K.H., Hughes, R.K., Piquerez, S.J., Jones, J.D., and Banfield, M.J. (2012). Distinct regions of the *Pseudomonas syringae* coiled-coil effector AvrRps4 are required for activation of immunity. Proc. Natl. Acad. Sci. USA **109:** 16371–16376.

Stegmann, M., Anderson, R.G., Ichimura, K., Pecenkova, T., Reuter, P., Žársky, V., McDowell, J.M., Shirasu, K., and Trujillo, M. (2012). The ubiquitin ligase PUB22 targets a subunit of the exocyst complex required for PAMP-triggered responses in Arabidopsis. Plant Cell **24:** 4703–4716.

Stuttmann, J., Peine, N., Garcia, A.V., Wagner, C., Choudhury, S.R., Wang, Y., James, G.V., Griebel, T., Alcázar, R., Tsuda, K., Schneeberger, K., and Parker, J.E. (2016). *Arabidopsis thaliana* DM2h (R8) within the Landsberg RPP1-like resistance locus underlies three different cases of EDS1-conditioned autoimmunity. PLoS Genet. **12:** e1005990.

Sukarta, O.C.A., Slootweg, E.J., and Goverse, A. (2016). Structure-informed insights for NLR functioning in plant immunity. Semin. Cell Dev. Biol. **56:** 134–149.

Sureshkumar, S., Dent, C., Seleznev, A., Tasset, C., and Balasubramanian, S. (2016). Nonsense-mediated mRNA decay modulates FLM-dependent thermosensory flowering response in Arabidopsis. Nat. Plants **2:** 16055.

Takahashi, S., Araki, Y., Ohya, Y., Sakuno, T., Hoshino, S., Kontani, K., Nishina, H., and Katada, T. (2008). Upf1 potentially serves as a RING-related E3 ubiquitin ligase via its association with Upf3 in yeast. RNA **14:** 1950–1958.

Thorvaldsdóttir, H., Robinson, J.T., and Mesirov, J.P. (2013). Integrative Genomics Viewer (IGV): High-performance genomics data visualization and exploration. Brief. Bioinform. **14:** 178–192.

Torres, M.A., Dangl, J.L., and Jones, J.D. (2002). Arabidopsis gp91phox homologues AtrbohD and AtrbohF are required for accumulation of reactive oxygen intermediates in the plant defense response. Proc. Natl. Acad. Sci. USA **99:** 517–522.

Trapnell, C., Williams, B.A., Pertea, G., Mortazavi, A., Kwan, G., van Baren, M.J., Salzberg, S.L., Wold, B.J., and Pachter, L. (2010). Transcript assembly and quantification by RNA-seq reveals unannotated transcripts and isoform switching during cell differentiation. Nat. Biotechnol. **28:** 511–515.

Trujillo, M., Ichimura, K., Casais, C., and Shirasu, K. (2008). Negative regulation of PAMP-triggered immunity by an E3 ubiquitin ligase triplet in Arabidopsis. Curr. Biol. **18:** 1396–1401.

van de Weyer, A.-L., Monteiro, F., Furzer, O.J., Nishimura, M.T., Cevik, V., Witek, K., Jones, J.D.G., Dangl, J.L., Weigel, D., and Bemm, F. (2019). A species-wide inventory of NLR genes and alleles in *Arabidopsis thaliana*. Cell **178:** 1260–1272.e14.

Wang, H., Ngwenyama, N., Liu, Y., Walker, J.C., and Zhang, S. (2007). Stomatal development and patterning are regulated by environmentally responsive mitogen-activated protein kinases in Arabidopsis. Plant Cell **19:** 63–73.

Wang, Y., Bao, Z., Zhu, Y., and Hua, J. (2009). Analysis of temperature modulation of plant defense against biotrophic microbes. Mol. Plant Microbe Interact. **22:** 498–506.

Wu, C.H., Abd-El-Haliem, A., Bozkurt, T.O., Belhaj, K., Terauchi, R., Vossen, J.H., and Kamoun, S. (2017). NLR network mediates immunity to diverse plant pathogens. Proc. Natl. Acad. Sci. USA **114:** 8113–8118.

Xu, F., Xu, S., Wiermer, M., Zhang, Y., and Li, X. (2012). The cyclin L homolog MOS12 and the MOS4-associated complex are required for the proper splicing of plant resistance genes. Plant J. **70:** 916–928.

Yang, S., Tang, F., and Zhu, H. (2014). Alternative splicing in plant immunity. Int. J. Mol. Sci. **15:** 10424–10445.

Yi, H., and Richards, E.J. (2007). A cluster of disease resistance genes in Arabidopsis is coordinately regulated by transcriptional activation and RNA silencing. Plant Cell **19:** 2929–2939.

Yoine, M., Ohto, M.A., Onai, K., Mita, S., and Nakamura, K. (2006). The lba1 mutation of UPF1 RNA helicase involved in nonsense-mediated mRNA decay causes pleiotropic phenotypic changes and altered sugar signalling in Arabidopsis. Plant J. **47:** 49–62.

Zhai, J., et al. (2011). MicroRNAs as master regulators of the plant NB-LRR defense gene family via the production of phased, trans-acting siRNAs. Genes Dev. **25:** 2540–2553.

Zhang, X.C., and Gassmann, W. (2007). Alternative splicing and mRNA levels of the disease resistance gene RPS4 are induced during defense responses. Plant Physiol. **145:** 1577–1587.

Zhang, Y., Xia, R., Kuang, H., and Meyers, B.C. (2016). The diversification of plant NBS-LRR defense genes directs the evolution of microRNAs that target them. Mol. Biol. Evol. **33:** 2692–2705.

Supplemental Data	/content/suppl/2020/02/26/tpc.19.00631.DC2.html
References	This article cites 106 articles, 37 of which can be accessed free at: /content/32/4/1081.full.html#ref-list-1
Permissions	https://www.copyright.com/ccc/openurl.do?sid=pd_hw1532298X&issn=1532298X&WT.mc_id=pd_hw1532298X
eTOCs	Sign up for eTOCs at: http://www.plantcell.org/cgi/alerts/ctmain
CiteTrack Alerts	Sign up for CiteTrack Alerts at: http://www.plantcell.org/cgi/alerts/ctmain
Subscription Information	Subscription Information for *The Plant Cell* and *Plant Physiology* is available at: http://www.aspb.org/publications/subscriptions.cfm